

✓
②

NAVAL POSTGRADUATE SCHOOL Monterey, California

AD-A245 387



DTIC
ELECTE
FEB 04 1992
S B D

THESIS

MODIFICATION AND EXPERIMENTAL VALIDATION
OF A COMBINED OPTICAL AND COLLECTION PROBE
FOR SOLID PROPELLANT EXHAUST ANALYSIS

by

Lyle J. Kellman

MARCH 1991

Thesis Co-Advisors:

David W. Netzer
David Laredo

Approved for public release: Distribution is unlimited

92-02633

Unclassified

SECURITY CLASSIFICATION OF THIS PAGE

REPORT DOCUMENTATION PAGE				Form Approved OMB No 0704-0188	
1a. REPORT SECURITY CLASSIFICATION Unclassified		1b. RESTRICTIVE MARKINGS			
2a. SECURITY CLASSIFICATION AUTHORITY		3. DISTRIBUTION/AVAILABILITY OF REPORT Approved for public release: Distribution is unlimited			
2b. DECLASSIFICATION/DOWNGRADING SCHEDULE					
4. PERFORMING ORGANIZATION REPORT NUMBER(S)		5. MONITORING ORGANIZATION REPORT NUMBER(S)			
6a. NAME OF PERFORMING ORGANIZATION Naval Postgraduate School		6b. OFFICE SYMBOL (if applicable) AA	7a. NAME OF MONITORING ORGANIZATION Naval Postgraduate School		
6c. ADDRESS (City, State and ZIP Code) Monterey, CA 93943-5000		7b. ADDRESS (City, State, and ZIP Code) Monterey, CA 93943-5000			
8a. NAME OF FUNDING/SPONSORING ORGANIZATION Air Force Phillips Laboratory		8b. OFFICE SYMBOL (if applicable)	9. PROCUREMENT INSTRUMENT IDENTIFICATION NUMBER		
8c. ADDRESS (City, State, and ZIP Code) Edward Air Force Base California		10. SOURCE OF FUNDING NUMBER	PROGRAM ELEMENT NO. F04611	PROJECT NO. 91-X-0072	TASK NO.
			WORK UNIT ACCESSION NO.		
11. TITLE (Include Security Classification) MODIFICATION AND EXPERIMENTAL VALIDATION OF A COMBINED OPTICAL AND COLLECTION PROBE FOR SOLID PROPELLANT EXHAUST ANALYSIS					
12. PERSONAL AUTHORS LYLE J. KELLMAN					
13a. TYPE OF REPORT Master's Thesis		13b. TIME COVERED FROM _____ TO _____		14. DATE OF REPORT (Year, Month, Day) MARCH 1991	15. PAGE COUNT 89
16. SUPPLEMENTARY NOTATION The views expressed are those of the author and do not reflect the official policy or position of the Department of Defense or the U.S. Government					
17. COSATI CODES			18. SUBJECT TERMS (Continue on reverse if necessary and identify by block numbers)		
FIELD	GROUP	SUB-GROUP	solid propellant rockets, particle sizing probe		
19. ABSTRACT (Continue on reverse if necessary and identify by block numbers) A combined optical and collection particle sizing probe was further developed and utilized for in situ measurements in the exhaust plumes of solid propellant rocket motors. Probe shock-swallowing capabilities were verified using schlieren observations under restricted motor operating conditions. Particle size number distributions obtained optically using a Malvern Mastersizer and from an automated data retrieval system for scanning electron microscope photographs of collected particles were in good agreement when referenced to common measurement limits. Most of the particles were smaller than 0.5μ, but a significant number were present with diameters to 10μ. A very few particles larger than 15μ were also present, some as single particles and some as agglomerates. SEM results showed that many particles were smaller than 0.2μ, outside the measurement range of the Malvern instrument. Suggestions are made for further improvements and validation procedures for the probe.					
20. DISTRIBUTION/AVAILABILITY OF ABSTRACT <input checked="" type="checkbox"/> UNCLASSIFIED/UNLIMITED <input type="checkbox"/> SAME AS RPT <input type="checkbox"/> DTIC USERS			21. ABSTRACT SECURITY CLASSIFICATION unclassified		
22a. NAME OF RESPONSIBLE INDIVIDUAL D.W. Netzer			22b. TELEPHONE (Include Area Code) (408) 646-2980	22c. OFFICE SYMBOL AA/Nt	

Approved for public release: Distribution is unlimited

Modification and Experimental Validation
of a Combined Optical and Collection Probe
for Solid Propellant Exhaust Analysis

by

Lyle J. Kellman
Captain, United States Army
B.S., United States Military Academy, 1982

Submitted in partial fulfillment of the
requirements for the degree of

MASTER OF SCIENCE IN
ASTRONAUTICAL ENGINEERING

from the

NAVAL POSTGRADUATE SCHOOL

MARCH 1991

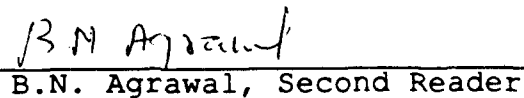
Author:

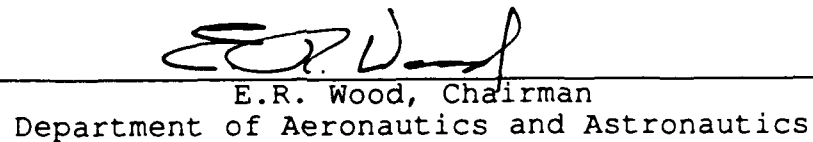

Lyle J. Kellman

Approved by:


D.W. Netzer, Co-Advisor


D. Laredo, Co-Advisor


B.N. Agrawal, Second Reader


E.R. Wood, Chairman
Department of Aeronautics and Astronautics

ABSTRACT

A combined optical and collection particle sizing probe was further developed and utilized for in situ measurements in the exhaust plumes of solid propellant rocket motors. Probe shock-swallowing capabilities were verified using schlieren observations under restricted motor operating conditions. Particle size number distributions obtained optically using a Malvern Mastersizer and from an automated data retrieval system for scanning electron microscope photographs of collected particles were in good agreement when referenced to common measurement limits. Most of the particles were smaller than 0.5μ , but a significant number were present with diameters to 10μ . A very few particles larger than 15μ were also present, some as single particles and some as agglomerates. SEM results showed that many particles were smaller than 0.2μ , outside the measurement range of the Malvern instrument. Suggestions are made for further improvements and validation procedures for the probe.



Accession For	
NTIS GRA&I	<input checked="" type="checkbox"/>
DTIC TAB	<input type="checkbox"/>
Unannounced	<input type="checkbox"/>
Justification	
Re	
Distribution/	
Availability Codes	
Dist	Avail and/or Special
A-1	

TABLE OF CONTENTS

I.	INTRODUCTION	1
II.	EXPERIMENTAL APPARATUS	7
	A. BACKGROUND	7
	B. EQUIPMENT	7
	1. Three Dimensional Subscale Motor	7
	2. Flow Deflection Device	9
	3. MALVERN Mastersizer	10
	4. MALVERN "Coffin" and Plume Splitter	13
	5. Particle Collection Probe	14
	6. Scanning Electron Microscope	15
	7. Automated Sizing System	16
	8. Schlieren System	17
	9. Automated Firing and Data Collection	17
III.	EXPERIMENTAL PROCEDURE	19
	A. COLD FLOW EXPERIMENTS	19
	1. Schlieren Examination	19
	2. Window Purge	20
	B. PRE-FIRING PROCEDURE	21
	C. COLLECTION MEASUREMENTS	23
	1. Scanning Electron Microscope	23
	2. Filter Paper in Solution	23
IV.	RESULTS AND DISCUSSION	25
	A. COLD FLOW EXPERIMENTS	25
	1. Schlieren Examination	25
	2. Window Purge	27
	B. TEST FIRINGS	28
V.	CONCLUSIONS AND RECOMMENDATIONS	35
	APPENDIX A: DESIGN DRAWINGS	38
	APPENDIX B: TABLES	42
	APPENDIX C: FIGURES	48
	APPENDIX D: MICROPEP OUTPUT	73
	LIST OF REFERENCES	78
	INITIAL DISTRIBUTION LIST	80

LIST OF TABLES

TABLE I.	VARIATION BETWEEN GAS AND SOLID PRODUCTS IN TWO PHASE FLOW LOSS [Ref. 1,p 376].	42
TABLE II.	CHARACTERISTICS OF SOLID PROPELLANT DD5 (AFAL) AND SHUTTLE PROPELLANT (Morton Thiokol)	43
TABLE III.	LABTECH NOTEBOOK CHANNEL ASSIGNMENTS	44
TABLE IV.	LINEAR REGRESSION OF TRANSDUCER CALIBRATION	45
TABLE V.	MOTOR AND PROBE RESULTS	46
TABLE VI.	MALVERN AND SEM PARTICLE SIZE DATA FROM VOLUME AND NUMBER DISTRIBUTIONS	47

LIST OF FIGURES

Figure 1.1.	Sequence of Computer Codes in the Calculation of Rocket Motor Performance and Plume Signature.	48
Figure 2.1.	Three Dimensional Subscale Motor. [Ref. 8].	49
Figure 2.2.	Malvern Light Scattering Principle [Ref. 11, p. 1-16].	50
Figure 2.3.	Malvern Enclosure and Plume Splitter.	51
Figure 2.4.	Probe Before Modification.	52
Figure 2.5.	Probe After Modification.	53
Figure 2.6.	Malvern Enclosure Interaction With Plume.	54
Figure 2.7.	Labtech Notebook Firing/Data Control. The Sequence of Triggering Which Follow Purge at $t=0$ are (a) Measure Background, (b) Ignition, (c) Deflector Down, (d) Measure Sample, and (e) Deflector Up.	55
Figure 3.1.	Pressure Calibration of Transducer During Pre-fire Check.	56
Figure 4.1.	Schlieren of Supersonic Nozzle Exhaust Flow Into Probe Tip.	57
Figure 4.2.	Schlieren of Probe Flow with 8° Half-Angle Wedge Located within the Measurement Volume.	58
Figure 4.3.	SEM Photographs of Collected Particles From Test 3-08.	59
Figure 4.4.	Example of Large Agglomerate from Test 3-12.	60

Figure 4.5.	Number Distributions for Test 2-14 Obtained from SEM Photographs of Collected Particles and from Measurements Using the Malvern Mastersizer.	61
Figure 4.6.	Number Distributions for Test 2-14 Obtained from Photographs of Collected Particles and from In Situ Measurements Using the Malvern Mastersizer, for Particles in Common Measurement Range.	62
Figure 4.7.	Number Distributions for Test 2-26 Obtained from SEM Photographs of Collected Particles and from Measurements Using the Malvern Mastersizer.	63
Figure 4.8.	Number Distributions for Test 2-26 Obtained from Photographs of Collected Particles and from In Situ Measurements Using the Malvern Mastersizer, for Particles in Common Measurement Range.	64
Figure 4.9.	Number Distributions for Test 2-28 Obtained from SEM Photographs of Collected Particles and from Measurements Using the Malvern Mastersizer.	65
Figure 4.10.	Number Distributions for Test 2-28 Obtained from Photographs of Collected Particles and from In Situ Measurements Using the Malvern Mastersizer, for Particles in Common Measurement Range.	66

Figure 4.11.	Number Distributions for Test 3-08 Obtained from SEM Photographs of Collected Particles and from Measurements Using the Malvern Mastersizer.	67
Figure 4.12.	Number Distributions for Test 3-08 Obtained from Photographs of Collected Particles and from In Situ Measurements Using the Malvern Mastersizer, for Particles in Common Measurement Range.	68
Figure 4.13.	Number Distributions for Test 3-12 Obtained from SEM Photographs of Collected Particles and from Measurements Using the Malvern Mastersizer.	69
Figure 4.14.	Number Distributions for Test 3-12 Obtained from Photographs of Collected Particles and from In Situ Measurements Using the Malvern Mastersizer, for Particles in Common Measurement Range.	70
Figure 4.15.	Number Distributions for Test 3-14 Obtained from SEM Photographs of Collected Particles and from Measurements Using the Malvern Mastersizer.	71
Figure 4.16.	Number Distributions for Test 3-14 Obtained from Photographs of Collected Particles and from In Situ Measurements Using the Malvern Mastersizer, for Particles in Common Measurement Range.	72

I. INTRODUCTION

Metals such as aluminum increase the performance of solid rocket motors when tactical requirements do not restrict exhaust plume signatures. Aluminum can boost the specific impulse of the rocket by augmenting the chemical energy of the combustion process. Aluminum also increases the stability of the combustion process by damping the higher frequency oscillations in the combustion chamber.

When a solid propellant is augmented with aluminum, the exhaust environment is complicated by the phenomenon of two-phase flow interactions between the gases and remaining solid particles from the products of combustion. The two-phase losses are due to the lag in velocity and temperature between the particles and the gas. Table I lists typical predictions of the variations in velocity and temperature between the gaseous and solid products of combustion of an aluminumized propellant in a motor with exit plane conditions of velocity = 9000 ft/sec and temperature = 2000°K [Ref. 1].

Predicting the performance of rocket motor designs and the propellants utilized, is accomplished using a series of computer codes. The actual process which occurs throughout the rocket motor environment from combustion chamber to the exhaust plume farfield must be separated into regions because of the complexity of the processes. Each of the regions has a

corresponding computer code which has been developed to predict the flowfield behavior. The complete series of computer program calculations is discussed in Ref. 2 and depicted in Figure 1.1. The NASA ODE or Naval Weapons Center PEP code provide the equilibrium compositions at the nozzle entrance, throat, and exit for one dimensional flow. However, no information is available from the code which can be used to determine the condensed material particle size distribution. The Solid Propellant Rocket Motor Performance (SPP) computer program [Ref. 2] incorporates the OD3P code for calculating the particle behavior through the nozzle. Particle collisions and breakup are calculated and the nozzle losses are calculated with semi-empirical methods. However, the particle sizes entering the nozzle are generally not known. Thus, in order to estimate the two-phase flow losses, the SPP code incorporates an empirical equation based upon the mass mean particle size (D_{43}) of the exhaust particles. The latter has been determined empirically by Hermsen [Ref. 3], but the standard deviation of the mass weighted average diameter for highly aluminized propellants had a correlation of not better than 35% [Ref 3, p.488]. If the particle size distribution at the nozzle entrance and exit could be experimentally determined, the accuracy of the SPP particle calculations could be determined. The JANNAF Standard Plume Flowfield Model (SPF) calculates the particle and gas distributions in the plume. However, the particle size distribution at the nozzle

exit (largely unknown) is needed for input. SPP output is not normally used for this data because it has not been validated. If the error in the input from SPP is significant then the output from SPF would cascade into the input for the Standardized Infrared Radiation Model (SIRRM [Refs. 2,4]).

With the increase in the technological advancement in the area of infrared imaging and the use of this technology to identify and target hostile ballistic projectiles, the need for an accurate prediction of the exhaust plume flowfield is essential. The characterization and measurement of the particle distribution and infrared/radiation signature of the exhaust plume of a solid propellant motor utilizing metalized propellants are difficult due to the dynamic and volatile nature of the exhaust plume.

Two methods which measure particle sizes in plumes are optical (light scattering or transmission) and particle collection. For full scale motors which use propellants with high concentrations of aluminum (i.e. 16%), the exhaust plume is extremely difficult to study optically due to multiple light scattering by the particles and extinction of the beam. To overcome these problems a combined optical and particle collection probe was designed to isolate a small stream of the plume [Ref. 5].

The goal of the particle collection portion of the probe design initiated by Eno [Ref. 5] was to overcome four basic problems encountered in the collection of exhaust particles:

1. the possibility of bias of the sample by disturbing the flow in the stream tube to be captured;
2. the possibility of particle entrainment effects from the atmosphere which can introduce foreign particles into the sample;
3. agglomerates of smaller particles or larger particles may be broken up during collection and/or subsequent handling; and
4. particles may continue to react after they have been captured, thus obscuring the true size and nature of the particles in the plume [Ref. 5].

In an attempt to overcome these problems Eno initiated the design of a combined optical and collection probe for use with sub-scale motors; based on a supersonic shock swallowing probe designed by the Air Force Rocket Propulsion Laboratory (AFRPL) [Ref. 6] and utilized in the research done by Hovland [Ref. 7]. The purpose of Eno's design was to accomplish the following;

1. capture a supersonic stream tube of the exhaust plume through the use of a shock swallowing tip modeled on that of the AFRPL probe;
2. measure the size distribution of the captured plume particles in situ through the use of a MALVERN Mastersizer particle sizing apparatus; and
3. collect the captured particles to examine their size distribution and compare it to the observations made in the stream tube by the Mastersizer [Ref. 5].

The possibility for using the Mastersizer was validated. Eno's effort resulted in a probe design which was successfully utilized in the plume for a propellant containing 16%

aluminum. It was demonstrated that the Malvern Mastersizer could be used with the probe and that the probe integrity could be maintained if exposure to the exhaust flow was limited to approximately one second. However, the following recommendations were made to further the design and validation of the probe system;

1. Investigate the shock pattern around the tip of the collection probe to determine if the changes made to the annular ejector flow (used to create a low backpressure within the probe and to prevent the particle flow from contacting the viewing windows) have any effect on the shock swallowing capabilities of the tip. This should be accomplished for various positions behind the exhaust nozzle, and varying degrees of over- and under-expansion.
2. Determine if the mass flow rates of the window purge and ejector are satisfactory for a variety of motor operating conditions.
3. Determine mass flowrate requirements at the exhaust plane of the probe which would allow the design of a diffuser for closed system collection of exhaust constituents [Ref. 5].

Based on the results and recommendations of Eno the following tasks were proposed for this investigation:

1. Utilize cold flow from the motor, schlieren photography and a video recorder to determine the effects of the nozzle exhaust pressure and the plume position on the shock swallowing capabilities of the probe tip.
2. Optimize the probe ejector flowrate, i.e. study the effects of the ejector flow on the detection capabilities of the Mastersizer and beam steering and record the results utilizing schlieren photography and a video recorder.

3. Design a diffuser for the aft end of the probe to allow for the collection of particles in a closed environment.
4. Utilize a scanning electron microscope (SEM) to study the collected particles. Determine a means to use the results from the SEM to correlate with the data obtained optically using the Mastersizer.
5. Consolidate the test procedure so that all aspects of the firing procedure can be controlled by the laboratory computer systems.
6. Design a test apparatus which will properly protect the collection probe and the Mastersizer from the extreme environment of the motor firing.
7. Use the probe at two different radial positions in the plume in order to;
 - (1) correlate/validate the optical and collected particle size data, and
 - (2) determine if significant changes in the particle size distribution occur in the radial direction within the plume (as expected from plume code predictions).

II. EXPERIMENTAL APPARATUS

A. BACKGROUND

A three dimensional subscale motor, a flow deflection device (to divert the flow away from the probe tip), a combined optical and particle collection probe, a Malvern Mastersizer particle sizing apparatus, a probe mount and a Mastersizer protection enclosure comprised the equipment required to conduct the tests. In addition, photographs were taken of the collected exhaust particles with a scanning electron microscope. In a related investigation a video scanner/image processing apparatus provided particle size distributions from the SEM photographs.

B. EQUIPMENT

1. Three Dimensional Subscale Motor

The solid propellant rocket motor used in this investigation was the same as used in the experiments conducted by Pruitt [Ref. 8], Youngborg [Ref. 9], and Eno [Ref. 5]. The diameter of the combustion chamber was 2.00 inches with a length of 10 inches. This motor was originally designed for the study of particle distributions at the entrance plane to the nozzle of the motor. It utilized nitrogen-purged viewing windows (Figure 2.1). These window mounting holes were plugged with stainless steel plates and

the nitrogen purge lines were capped. Study of particle distributions inside the motor continues on another investigation. To permit both investigations to be conducted concurrently a new motor was designed without windows. The new motor could not be fabricated for this investigation, but should be available for subsequent investigations. The nozzle throat diameters for the motor were sized based on the burning characteristics of the propellants and the desired chamber pressure within the motor. The two propellants studied contained 4.69% and 16% aluminum. Table II lists the compositions of the propellants and their burning characteristics. The propellant grain size in the motor was 1.99 inches in diameter and 1.00 to 1.50 inches thick. The end-burning propellant grain was loaded in the motor utilizing a self vulcanizing silicone rubber compound (RTV). The weight of the propellant varied from 80 to 100 grams.

The area of the throat (A^*) of the nozzle was calculated with the following steady state equation,

$$P_c = (A_b * C^* * a * \rho / A^*)^{1/1-n} \quad (1)$$

where

P_c =chamber pressure a = propellant constant

A_b =propellant burn area ρ = propellant density

A^* =nozzle throat area

n = propellant burning rate exponent

C^* =characteristic velocity for the propellant

C^* is taken from the computer program MICROPEP. Examples of the MICROPEP output are found at Appendix D. For a desired chamber pressure and the propellant values from Table II, A_e can be calculated for one-dimensional, fixed property, isentropic flow with the following;

$$\frac{P_c}{P_e} = \left(1 + \frac{\gamma-1}{2} M_e^2\right)^{\frac{\gamma}{\gamma-1}} \quad (2)$$

$$\frac{A_e}{A^*} = \frac{1}{M_e} \left[\frac{1 + \frac{\gamma-1}{2} M_e^2}{\frac{\gamma+1}{2}} \right]^{\frac{\gamma+1}{2(\gamma-1)}} \quad (3)$$

Where

M_e = nozzle exit mach number

A_e = nozzle exit area

P_e = static pressure at the nozzle exit

For a desired degree of overexpansion ($P_e < \text{ambient pressure}$) or underexpansion ($P_e > \text{ambient pressure}$) P_e is known. Equation (2) yields M_e and Equation (3) then yields the required nozzle area ratio. Only underexpanded exhaust jets were utilized in the present investigation. The nozzles were made of copper. To ignite the motor, a half-inch bolt was hollowed out and loaded with BKNO_3 . The BKNO_3 was ignited with a nichrome wire filament energized by a 12 volt power source.

2. Flow Deflection Device

The deflection device served two purposes. First, when the probe and Mastersizer are placed in the volatile

environment of the exhaust plume, the exposure time must be kept to a minimum to prevent damage due to the extreme temperatures. The exposure time was limited to 0.7 secs. The second purpose of the deflection device was to delay the exposure of the probe and Mastersizer until the motor was operating at steady-state conditions to prevent contamination of the collected sample from the products of the ignition. The flow deflection device which was originally designed by Eno limited the placement of the collection probe and the Mastersizer to distances which allowed data collection only in the plume farfield (>40 nozzle diameters) [Ref. 5]. The deflection device used in this investigation was made smaller to enable data collection in either the plume farfield or the plume nearfield (at distances of 4 to 10 nozzle diameters). The deflector device was actuated via an air pressurized pneumatic piston and valve, which was triggered by a 110 volt solenoid. Control of the deflection device was provided from the control room computer utilizing Labtech Notebook software.

3. MALVERN Mastersizer

The MALVERN Mastersizer [Ref. 10] used for this investigation was the same as that used by Eno [Ref. 5]. It is a commercially designed and produced laser system utilizing forward scattering of an incident collimated laser beam to determine particle size distributions. Figure 2.2 is a representation of the principles governing the software

provided with the Mastersizer. The software is proprietary in nature and is not available for modification.

The Mastersizer system uses a 2mW helium-neon laser (.6328 micron wavelength), with beam expansion to 18 millimeters. The entire system is self supporting and mounted on an integrated optical bench which allows the use of various accompanying specimen handling devices. The system has three lens options with focal lengths of 45, 100, and 300 millimeters (mm). For this investigation the 100 mm lens was used for the motor firing experiments and data collection. The 100 mm lens is used as a Fourier transform lens and can measure particles in the range of 0.5- 170 microns. When the filter paper which is used for particle collection is dissolved in acetone, it provides particles in solution vs. in gas. In this case the 45 mm lens was used. The 45 mm lens is used as a reverse Fourier transform lens to study particles as small as 0.1 micron. It is used with a special presentation cell and a magnetic motor to stir the specimen within the cell. The dynamic range of each lens is 800:1 and the manufacturer claims an accuracy for the system of +/- 2% [Ref. 10]. Eno, as part of his investigation, validated the capabilities of the Mastersizer using polystyrene particles of known mean diameter. His results are summarized below:

1. Particles below the resolution limit of the 100 mm lens (0.5 microns), but above approximately 0.25 microns affected both the measured distribution and the calculated mean diameters in a significant

manner. Particles below this size had only a small effect on the calculated distributions.

2. Large changes in the specified absorptive index had a significant effect on the calculated particle distributions. However, for the range of values of differential refractive index (DRI) and sample absorptive index (Ua) expected to be encountered in the exhaust plumes of aluminized propellants, negligible effect on the derived distributions can be expected [Ref. 5].

To determine the particle distributions the Mastersizer uses a 31 element solid state detector array consisting of 31 individual chips mounted in a single pie-shaped array. The chips are sampled in parallel through individual amplifiers. The Mastersizer software allows for the sampling of all 31 detectors in 12 milliseconds (ms). This 12 ms sampling is termed a sweep. The system will allow from one to 32768 sweeps, which are averaged and used for the calculation of the particle distribution.

The Mastersizer allows for various inputs of the differential refractive index and absorptive index. The values which can be used are taken from a table in the instruction manual. The appropriate values are determined by the user, based on the characteristics of the anticipated particle composition. The forward scattering is measured to an angle of 50°. The system allows for Mie corrections to the Fraunhofer diffraction theory, permitting particles in gas as small as 0.5 microns to be measured. The system will measure multimodal distributions.

4. MALVERN "Coffin" and Plume Splitter

During the experiments conducted by Eno [Ref. 5], the probe was placed far enough away from the motor exit that the severe heat was dissipated before reaching the original enclosure for the Mastersizer. During cold flow experiments of the current investigation, the need for placing the Mastersizer closer to the motor exit was determined (the findings of the cold flow experiments are discussed in chapter III). The Mastersizer was previously placed in a box made of aluminum, which had the primary purpose of protecting the Mastersizer in the event of an explosion of the motor. When the Mastersizer was placed less than four inches from the motor exit, the heat from the combustion and exhaust process melted through the aluminum box and could have caused severe damage to the Mastersizer. To protect the Mastersizer from the heat of the motor the MALVERN "coffin" was constructed (see Appendix A), and is pictured in Figure 2.3. The "coffin" was designed in two parts, the main body, and the probe mount and plume channel. The main body was made of 1/8 inch thick aluminum, welded at the seams. The plume channel was made of 1/8 inch thick stainless steel, welded at the seams. The plume channel was modified with plume splitter plates to capture the plume far in front of the "coffin" and prevent plume distortion at the probe tip. The plume splitters were also made of stainless steel, and attached to the plume channel as pictured in Figure 2.3.

5. Particle Collection Probe

The particle collection probe was designed by Eno [Ref. 5] to emulate some of the features of the AFRPL probe (see Appendix A). The probe was designed to be used in conjunction with the Mastersizer to obtain in situ measurements of the particles in the exhaust of a solid propellant rocket motor. The probe was designed to isolate a small stream tube of particles from a rocket plume exhaust to allow the Mastersizer to measure a particle distribution with a minimal disturbance to the captured flow. This is accomplished by the probe tip by swallowing the flow without introducing any strong shocks at the probe tip entrance. Once the flow is inside the probe it is viewed via two windows. The input window is only large enough to pass the 18 mm diameter laser beam. The output window is much larger to accommodate the forward scattered light to angles of 50° . The windows are kept clear by injecting an annular dry nitrogen flow around the particle laden stream tube to restrict it from expanding until it passes past the windows. An additional flow is injected above the entrance to the measurement volume to prevent recirculation and to purge the larger window. Eno's experiments proved the possibility for the use of the probe in its original configuration, but modifications needed to be made to make the probe reliable as a data collection device.

The first modification made was to the aft end of the probe body to allow for the use of 0.25 micron millipore

filter paper for the collection of the exhaust products. The original design had a 1.4 x 0.4 inch rectangular piece of filter paper mounted at the end of the probe. This configuration caused a build-up of back pressure, which caused the filter paper to be blown from the probe. The modification which was designed to overcome this problem was an extension to the aft end of the probe to allow for the flow to diffuse to accomplish two purposes (Appendix A). The first was to decrease the velocity of the flow at the filter paper. The second was to decrease the build-up of pressure within the probe. The filter paper is now mounted on an apparatus which allows the use of a 1.62 inch diameter circular flow. The before and after modification illustrations of the probe are found in Figures 2.4 and 2.5.

The second modification was the design of a probe tip extension. The probe is mounted on the Mastersizer coffin at a position which can introduce undesirable circulation and turbulence to the plume exhaust (Figure 2.6). The tip extension was designed to be placed at the entrance to the probe to extend it forward, past the corner which introduces the turbulence. However, time restraints did not permit it to be employed in the present investigation.

6. Scanning Electron Microscope

The scanning electron microscope employed was a Hitachi S-450 model, operating with a maximum current of 200

μA The voltage range was 2-30 Kv. The resolution was 60\AA with a magnification range from 20 to 200,000 [Ref. 11]. Specimens are fixed to a 0.5 inch aluminum pedestal, dehydrated, and critical point dried. They are then coated with a 100 atom thick ($4\text{E}-10$ inches) layer of gold.

An image is produced on a cathode ray tube which is photographed with a conventional camera using Polaroid Polapan 52, 4x5 inch instant sheet, medium contrast black and white film, ISO 400/27°.

7. Automated Sizing System

The automated sizing system developed on another investigation [Ref. 12] consisted of an IBM AT microcomputer fitted with dedicated hardware, and run by a program written in C language.

The photographs taken with the SEM are processed into the system via a vidicon camera and then digitized with a frame grabber. The digitized image is processed by the microcomputer and displayed on a video monitor. A detailed description of the hardware configuration is discussed by Lee [Ref. 12]. Lee incorporated various commercially produced software programs in addition to the locally written SEMEX program in C language as partial fulfillment of his thesis. The output of his program is a particle distribution based on the pictures from the SEM. The results were configured in the

same format as that of the Mastersizer for ease of comparison of the optical and collected particle size data.

8. Schlieren System

A schlieren system was used to study the flow phenomenon at the tip of the collection probe and within the measurement volume, to determine the limiting operating pressures and Mach numbers of the apparatus.

The system used a 120 volt mercury arc lamp as a light source. A double knife-edge slit was placed 10.5 inches away from the arc lamp at the point where the light could be focused to a pinpoint. 25.2 inches from this point a 6 inch diameter lens was placed to collimate the light beam. An identical lens was placed a distance of approximately 8 inches from the first lens to focus the light onto a single knife edge. A cross-hatched screen was used to focus the image of the tip and flowfield located between the two lenses. Flows from the motor and through the probe's window purge and ejector nozzle were provided using compressed air from the laboratory's air compressor.

9. Automated Firing and Data Collection

The complexity and short test time of the firing sequence and data collection required the development of a more advanced automated controlling system. Labtech Notebook is a commercially produced software program which can be customized to the requirements of the experiment. All aspects

of the firing and data collection are currently controlled via the Labtech Notebook software and a IBM/AT microcomputer. The channel assignments are listed in Table III and the timing of the firing and data collection are illustrated in Figure 2.7.

III. EXPERIMENTAL PROCEDURE

A. COLD FLOW EXPERIMENTS

1. Schlieren Examination

The schlieren system was used to conduct an extensive study of the shock swallowing capabilities of the probe. The probe was mounted at various positions behind the three dimensional motor and the chamber pressure was varied to determine the range of performance of the probe. The motor was fitted with a nozzle with an area ratio of 1.69, which produced an exit flow Mach number of 2, with ideally expanded flow when the chamber pressure was maintained at 115 psia.

The motor was first mounted without the probe and the chamber pressure was varied from 0 to 150 psia. The schlieren of the flow from the motor was then recorded with a video camera to determine the shock patterns in the exhaust plume corresponding to the set pressures. The flow aft of the motor was studied with the knife slit in both horizontal and vertical configurations. A Kiel probe was then placed in the flow of the plume to determine the losses in stagnation pressure as a function of distance from the nozzle exit.

The probe tip was then placed at various positions from 2 to 30 nozzle exit diameters away from the motor, to determine at what distances the shock could be swallowed. The

Kiel probe was then placed inside the probe to determine the pressure losses experienced inside the probe, from the tip to the optical measurement volume. The entire procedure was recorded on video.

The probe was then repositioned to study the flow behavior in the measurement volume under various operating conditions. To determine if the flow inside the probe remained supersonic, a knife edge was placed in the measurement volume and the flow was examined for the presence and angle of an oblique shock. The procedure was again recorded on video.

2. Window Purge

The flows injected into the measurement volume can introduce additional turbulence, which in turn can affect the measurements made by the Mastersizer. The principle problem that could occur was beam steering; the result of the high density gradients in the shear layer between the probe tip streamtube and the ejector flows. The probe was placed on the Malvern "coffin" in the hot-fire configuration and a simulation of flow into the probe from the motor was conducted using compressed air. A background measurement with no flow was first taken, followed by a sample taken of the air flow through the probe with no ejector flow. The procedure was repeated, with step increases in the ejector flow. Background and sample measurements were taken for each of the steps and

the results were analyzed for determination of the best operating conditions.

B. PRE-FIRING PROCEDURE

A series of steps were followed prior to the firing of the motor to ensure that all the data collection programs and devices were calibrated and working properly according to the firing time table.

A strain-gage pressure transducer, calibrated with a dead weight tester, measured the chamber pressure during the run. The tester was loaded from 0 to 800 psi in increments of 100 psi. The readings were recorded using the Labtech Notebook program to ensure that the program was properly working and to use the programs link to Lotus 123 program software to execute a linear regression analysis of the data. The latter calculated a calibration constant for the transducer. An example of the linear regression calculations are found in Table IV and the actual calibration curve and constant are graphically represented in Figure 3.1.

The Mastersizer was then placed in the Malvern "coffin" and the collection probe placed in the center section. The windows were mounted using teflon tape and an o-ring to ensure that there were no air leaks. The circular window was canted to eliminate reflections which could impinge on the diode array. A background measurement was taken with the Mastersizer to verify proper alignment of the beam on the detector diodes.

After a satisfactory background was measured the gaps and seams around the probe and Malvern "coffin" were sealed with RTV.

The motor was then mounted at a position from the collection probe determined by the requirements for the run (distance from the probe and radial position in the plume). The plume deflector moved with the motor position to ensure that the plume was deflected close to the nozzle exit. The pressure tap line and burst disk extension were then attached. The burst disk was utilized to provide a safety valve in the event of a plug occurring at the nozzle throat during the test. The burst disk was rated at 1000 psi, which was 2 ½ times the expected pressure for the motor.

The computer programs were then loaded, with the data to be saved in files named according to the date of the run. The Labtech Notebook program was outlined previously. The Malvern program was triggered to measure a pre-fire background, after the activation of the purge gas, but before the motor ignition. A sample measurement was taken during the motor firing. Post-fire background and sample measurements were taken 0.3 seconds and approximately 3.0, respectively, after the sample measurement, to determine the cleanliness of the windows.

Once all other preparatory steps were completed, the BKNO₃ ignitor was loaded. In the control room the video camera and IR imaging system were programmed. After the area had been

cleared for safety the Labtech Notebook program was initiated and the firing sequence outlined in Section II.B.9 executed.

C. COLLECTION MEASUREMENTS

1. Scanning Electron Microscope

After completion of the data run the filter paper was removed. Two 0.5 inch circular pieces were cut out (one from the center and one from the outer edge) and mounted on 0.5 inch diameter pedestals as outlined in Section II.B.6.

The specimen was first viewed with the SEM at a low magnification ($\approx 100-200 X$) for evidence of any large particles ($\approx 30-50$ microns). The magnification was then increased ($\approx 500-1500 X$) and particle groups found and photographed. 10-30 photographs were taken for each data run. The photographs were then analyzed as outlined in section II.B.7.

2. Filter Paper in Solution

The remaining filter paper was dissolved in a beaker of acetone and placed in an ultrasonic cleaner. The particles were allowed to settle for approximately 12 hours and excess solution was removed. Fresh solution was added and the process was repeated. The entire process was repeated until the majority of the products of combustion other than the Al_2O_3 were moved. The remaining solution was then placed in the special presentation cell for the 45 mm lens and analyzed by the Malvern Mastersizer. In general, this procedure was

unsatisfactory because the collected particle mass provided too low a concentration in liquid for the Mastersizer.

IV. RESULTS AND DISCUSSION

A. COLD FLOW EXPERIMENTS

1. Schlieren Examination

The video images revealed that the underexpanded flow aft of the motor experienced Prandtl-Meyer expansion at the nozzle exit, followed by a series of compression and expansion waves. The images also revealed that the first strong normal shock occurred at a distance of approximately 2 inches (or 5 nozzle exit diameters) aft of the nozzle exit. Based on these observations the probe would have to be placed upstream of this shock if nozzle exit plane particles were to be measured (without possible breakup caused by the shock). The results from the Kiel probe measurements further substantiated this optical observation. The Kiel probe, with a bow shock, recorded a pressure of 83 psia. Using normal shock tables the downstream pressure after a Mach 2 normal shock (upstream pressure of 115 psia) should be 83 psia. The losses from the nozzle exit plane to the probe location 2 nozzle exit diameters from the motor (0.766 inches) were negligible.

The schlieren observations revealed that a bow shock formed upstream of the tip at low motor pressures (Figure 4.1(b)). Under these conditions the exhaust nozzle was overexpanded and strong oblique shocks extended into the plume

upstream of the probe tip. This greatly reduced the Mach number at the probe tip. As the pressure in the motor was increased the bow shock slowly moved towards the tip, attached and was swallowed by the probe (Figure 4.1(c)). Small fluctuations in the pressure of the compressed air supply to the motor prevented clear pictures of the attached shock, but the swallowed shock condition was readily apparent.

The interior diameter of the probe tip diverged from 0.130 inches to 0.170 inches. Under isentropic conditions the flow would continue to expand and increase in velocity to Mach 2.9. A Kiel probe located in this ideal flow would form a normal shock, resulting in a downstream pressure of 41 psia (upstream pressure = 115 psia). However, the actual measured downstream pressure was 71 psia, indicating that the normal shock on the Kiel probe was weaker. Thus, oblique shock (and friction) losses within the probe tip resulted in the exit Mach number being less than 2.9. With no ejector flow or windows in the probe the probe tip exit flow exhausted into local ambient pressure. This resulted in a continued series of expansion and compression waves aft of the tip. When an $\approx 8^\circ$ wedge angle was placed in this flow at the center of the measurement volume, the shock angle was $\approx 50^\circ$ (Figure 4.2). These conditions corresponded to a Mach number of ≈ 1.6 . Thus, oblique shock losses exist within the probe tip flow channel. However, the flow remains supersonic without shockdown to subsonic conditions. Overall, the probe tip swallowed the

shock when the upstream Mach number was > 1.3 . For Mach numbers > 1.0 but < 1.3 , a weak bow shock formed upstream of the tip and should not affect the particles significantly.

2. Window Purge

The Mastersizer can most accurately measure particle size distributions when the background readings from the diodes are below a reference of 30. The density gradients created by the shear layer between the main flow (probe tip) and the ejector flows caused beam steering of the incident laser beam. This results in readings greater than 30 on the lower diode rings. When beam steering is present the voltages on the affected inner rings can be "killed". When the measurements were taken with no ejector flow the first eight diode rings were affected by beam steering. With the ejector stagnation pressure set at 50 psia, beam steering occurred on the first ten diode rings. An ejector pressure of 100 psia (with a motor pressure of 115 psia) resulted in the minimum beam steering (first six diode rings).

The optimum ejector pressure to minimize beam steering will depend upon the motor operating pressure and the probe location within the plume. In general, the minimum beam steering will occur when the velocities and pressures of the probe tip and the ejector flows are the same.

When the inner six diodes are not utilized in the determination of the particle size distribution, particles

larger than approximately 50 microns will not be measured. Fortunately, particles this large are not normally observed in exhaust plumes.

B. TEST FIRINGS

A total of nine tests were conducted. Three of the nine were unsuccessful due to either malfunctions in the test equipment or rapid burning of the propellant due to bonding irregularities. The six remaining tests will be referred to by number (i.e. 2-14) corresponding to the month and date of the test. Major results are presented in Tables V and VI. The Malvern data shown in Table V shows a lower size limit of 0.2 microns. The Mastersizer can accurately measure particles as small as 0.48 microns using the 100 mm lens. However, an estimate of the percentage of the particles within the range 0.2-0.48 microns is also included in the Mastersizer output data.

Particles as small as 0.05 microns were observed on the filter paper. The filter paper had passage areas that permitted 0.25 micron or smaller particles to pass through. Thus, only a portion of the particles smaller than 0.25 microns which impacted the filter paper were actually captured. Particles smaller than 0.13 microns were not counted due to limitations of the automated data processing technique (gray-shade threshold). Figure 4.3 shows typical SEM photographs from the test 3-08. Some of the largest particles

obtained from the SEM photographs were agglomerates as shown in Figure 4.4. It is not known where this agglomeration occurred.

In Table V the probe tip location is given as a distance from the nozzle exhaust in nozzle exit diameters. In all cases except for test 2-26, the plume flow at the tip location was subsonic. As discussed in section II.B.4 two splitter plates (except 3-12 which used only one splitter plate) were used to prevent the plume flow from being affected by the Malvern enclosure (horizontal plume mixing was prevented, whereas vertical plume mixing was permitted). Thus, the particle sizes measured may not be identical to those at the same location in an undisturbed plume. This was the reason for designing and fabricating the probe tip extension discussed in section II.B.5 (not used in the present investigation). In test 3-12 only the splitter plate attached to the corner of the Malvern enclosure was used. Thus, some horizontal mixing was also possible.

The particle sizes obtained from the SEM photographs should be representative of those measured optically. However, the size distributions may not be statistically valid even for test 3-08 in which 6427 particles were sized. For this test the probe should have collected ≈ 0.012 grams of condensed material (assuming all as Al_2O_3). The volume of the counted particles was $2725\mu^3$. Thus, the 40 images used to obtain the distribution represented only $\approx 5\text{E-}12$ grams ($4\text{E-}8\%$ of the

mass entering the probe). Assuming the particles were uniformly distributed on the filter paper, only $3E-8$ grams would be collected (0.00025% of the total mass entering the probe). Thus, most of the particles were deposited on the interior probe walls, passed through the filter paper (if $< 0.25\mu$), or around the filter paper holder. This was supported by the visible presence of particles on the interior probe walls. Some particles could possibly pass around the filter since the filter holder was slightly relieved to prevent pressure build-up within the probe. In addition, the larger particles probably were deposited on the lower probe surface before reaching the filter paper. The Malvern samples all of the probe flow for 0.3 seconds. Assuming an average diameter of 0.6μ (much larger than the average diameter from the SEM photographs), the Malvern would have measured $\approx 3E+6$ particles. Thus, the Malvern distribution was based upon ≈ 450 times as many particles as was the SEM distribution.

For all the tests the probe was positioned to measure the particles on the plume centerline. However, on tests 3-08 and 3-12, the plume exiting the nozzle was deflected, apparently from throat accumulations. This resulted in the probe measurements actually representative of the conditions radially displaced from the plume centerline.

Except for the first test which utilized 16% aluminum, all tests employed the same propellant (4.69% Al) at essentially the same chamber pressure. Each subsequent test attempted to

improve the quality and confidence in the particle size data. Most of the modifications evolved around trying to minimize window deposits.

As discussed above, the SEM data is based upon a very small sample size compared to the Malvern measurement. Therefore, very few (or even singular) large particles "seen" by the Malvern and not in the SEM photographs (large particles were probably deposited on the lower probe walls) would result in very large differences in the volume distribution. Conversely, when one or two large particles were seen in the SEM photographs they would completely dominate the volume distribution resulting in an artificial bias towards the large particle (for example: from a 543 particle sample, one 15 μ particle represented 52% of the volume). For this reason, number distributions were more meaningful for comparison of the Malvern and SEM data.

The minimum particle size bin used by the Malvern is 0.2-0.48 μ , whereas for the SEM data it was 0.13-0.16 μ . In addition, the Malvern generally showed that most of the particles were in the smallest size bin. Because of the low particle count obtained for the SEM data and possibly some built-in bias in the automated retrieval algorithm for the smaller particle sizes, the SEM data was also curve-fitted using a third-order polynomial. Therefore, the results from each test are presented in two number distribution plots. The first plot shows all of the SEM raw data and the curve-fit

together with the Malvern data; neglecting the point in the Malvern 0.2-0.48 μ particle bin in order to properly scale the graph. The second plot attempts a better comparison between the SEM and Malvern data. All particles less 0.2 μ microns were eliminated from the SEM data since the Malvern cannot detect them. All SEM particles between 0.2 and 0.48 μ (5 bins) were grouped together to emulate the smallest bin in the Malvern output. These results are depicted in Figures 4.5 - 4.16.

When utilizing the Malvern, several data analysis mode options are available. It is most desirable initially to select the Model Independent mode, since it permits multi-modal distributions to be detected. However, when a mono-modal distribution actually occurs, the model independent mode often does not properly curve-fit the raw voltage data. This is evidenced in the "display fit" option of the Malvern software and also by the "residual" which measures the difference between the curve-fit and raw data (Malvern recommends the residual be < 2.0).

The first two tests (2-14,2-26) used low window purge and ejector flowrates. Even though there was a reasonable match in the Malvern and SEM number distributions and size ranges (Table VI and Figures 4.6, 4.8), the Malvern "residual" was high and the window deposits were significant. Post-run Malvern measurements through these dirty windows resulted in diode voltage levels and a size distribution similar to those obtained during the test. The measurements could have been

good (obtained while the windows were clear), with the windows fowling after the Malvern measurement, or the measurements could have been made with the windows deposits in place. During the third test (2-28) the window purge rate was significantly increased. The residual for the Malvern curve-fit became acceptable (2.2%), but the window deposit problem persisted.

During the first three tests the probe tip exhausted 0.337 inches from the upstream edge of the circular window. It was felt that perhaps the flow from the tip spread too rapidly to the walls and windows. The probe tip was then modified to extend it to the upstream edge of the circular window. Plexiglas side plates were installed on the probe and an alcohol droplet spray was injected into the probe tip. The flow pattern was observed using a video camera. However, the results of the modification were inconclusive regarding any improvement in the jet spreading to the window surface.

Test four (3-08) was therefore conducted with the above modification, but without window purge or ejector flow. It was hoped that the jet would not spread to the windows and that recirculation within the probe volume would be reduced.

The Malvern residual was quite good (0.6%) and there was improvement in the window cleanliness. However, the post-run Malvern measurements continued to register levels higher than desired. During this test, nozzle deposits also resulted in

the exhaust plume being deflected, which resulted in the probe tip being in the edge of the plume.

The probe was again modified before test five and six (3-12, 3-14). Window purge was used, but without the ejector flow. In test 3-12 an attempt was made to permit additional horizontal plume mixing by removing one of the splitter plates. However, this resulted in skewing the Malvern distribution to peak near 2μ (vs. $< 0.48\mu$) and only a very few of the smaller particles (Figs 4.13 and 4.14). Apparently the subsonic flow near the probe tip was considerably deflected, resulting in the most of the smaller particles following the gas flow to the side of the probe tip. The SEM data continued to show the dominance of the smaller particles. This was further evidence that the larger particles entering the probe did not reach the filter paper, but rather were deposited on the lower walls.

Prior to test six (3-14), very careful alignment was used to ensure that the probe tip and motor nozzle centerlines were coincident. The signal strength for the Malvern diode during the test was quite large compared to the post-run measurement signals, indicating that the windows were comparatively clean and that the confidence in the size distribution obtained was quite high. Figure 4.16 also shows quite good agreement between the Malvern and SEM number distributions when both were based on the particle sizes detectable by the Malvern.

V. CONCLUSIONS AND RECOMMENDATIONS

The combined optical and collection probe was further developed and validated in this investigation. Cold-flow schlieren observations were used to determine the conditions under which the probe was capable of swallowing the bow shock when placed in the supersonic portion of the exhaust plume. The probe was shown to swallow the shock when the flow Mach number was > 1.3 . For $1.0 < M < 1.3$ a detached conical shock exists at the probe tip. This shock is quite weak and should not significantly alter the particle size distribution. The schlieren observations also showed that when the probe tip was located within a flow in which $M > 1.3$, the probe tip exhaust remained supersonic as it passed into the measurement volume. Optimum probe ejector flow depends upon the motor operating conditions and probe location within the plume. In general, to prevent beam steering of the Malvern laser it is desired to match the static pressures of the ejector and probe tip exhaust flows.

A computer controlled testing procedure was successfully used which properly controlled, timed, recorded and displayed the required events. In addition, a plume deflector was successfully utilized which could be placed directly behind the nozzle exhaust and could accurately limit the probe exposure time to the desired 0.7 seconds.

The procedure for the automated data retrieval (ADR) of particle size distributions from SEM photographs was significantly improved on a related investigation and successfully used to obtain number distribution plots from the particles collected in the probe. However, The SEM data can only be used for general comparison with the Malvern optical data because the sample size is extremely small (even for over 6000 particles). There also appears to be some bias in the ADR process which eliminates most particles with diameters of approximately 0.25μ . It is recommended that two tests be conducted under identical conditions, one using the Malvern and collection filter as in the present investigation. The second test should locate a series of filter paper holders very near the probe tip exhaust in order to capture most of the particles entering the probe and "seen" by the Malvern in the first test. Currently it is believed that most of the larger particles and many of the smallest particles are deposited on the internal surfaces of the probe. The filter papers should then have enough mass deposited upon them to permit use of the Malvern to measure the particle size distribution down to 0.1μ ; using dissolved filters and the particles in solution.

Splitter plates were used to prevent the Malvern enclosure from interfering with the plume flow before it reached the probe tip. However, these plates prevented most horizontal mixing and may have introduced oblique shocks when located

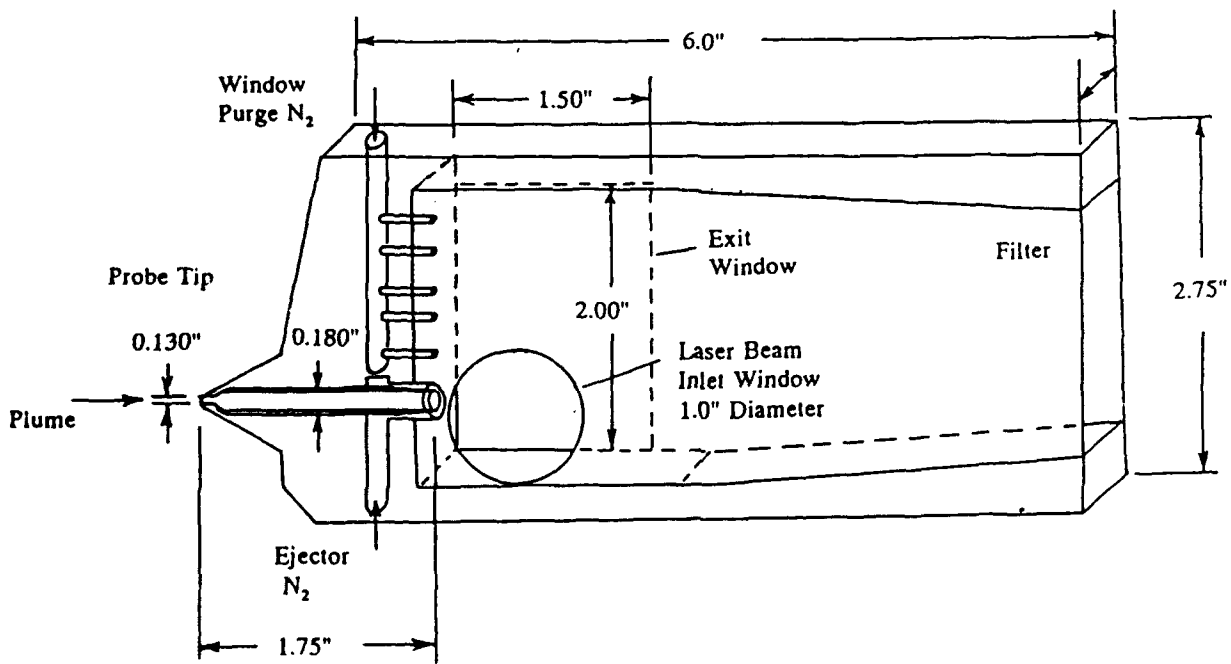
near the nozzle exhaust. They may, therefore, alter the particle sizes and bias the data. The probe tip extension designed and fabricated should be used in place of the splitter plates. However, proper shock swallowing will have to again be verified.

The probe design has evolved to the point where the windows can be kept quite clean, resulting in good agreement between the optical and collected particle size number distributions. The SEM data can be used to help identify the size and quantity of the particles which are below the 0.2μ measurement range of the Malvern.

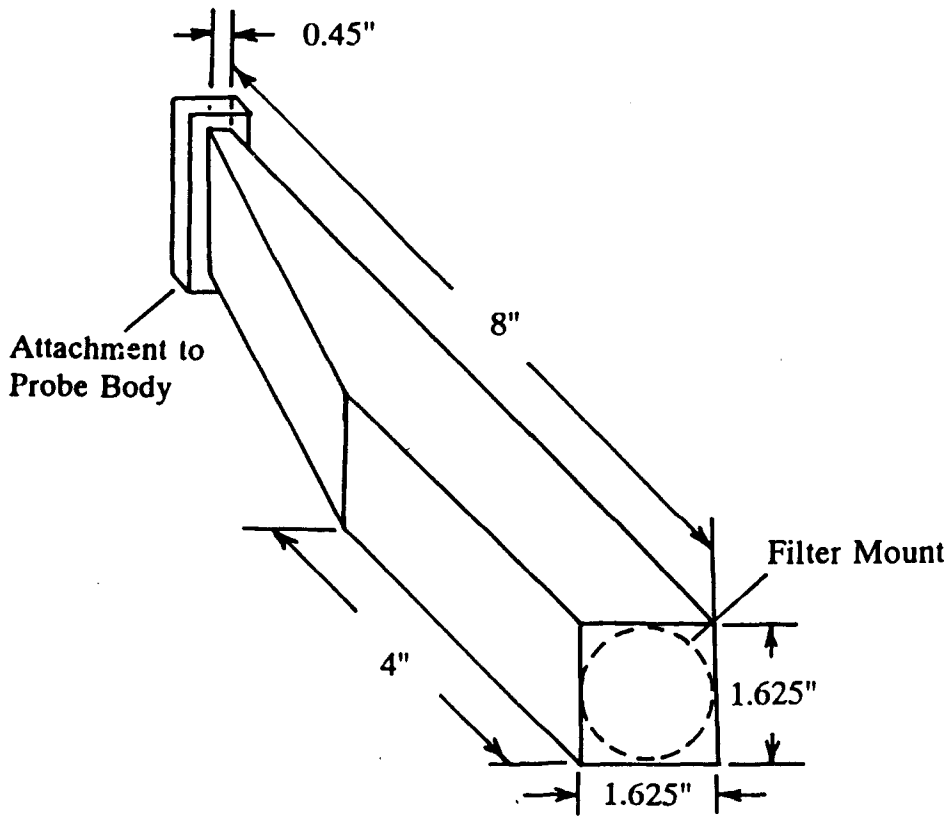
Most of the plume particles were smaller than 0.48μ , but a significant number were present with diameters to approximately 10μ . A very few extremely large ($>15\mu$) particles were also present, some being single spherical particles and other being agglomerates of many smaller particles.

It is recommended that the probe ejector flow again be utilized in conjunction with the present probe configuration. In addition, probe validation should be continued using inert exhaust particles of known distribution for determination of measurement accuracy and a better comparison between the SEM and Malvern size distributions.

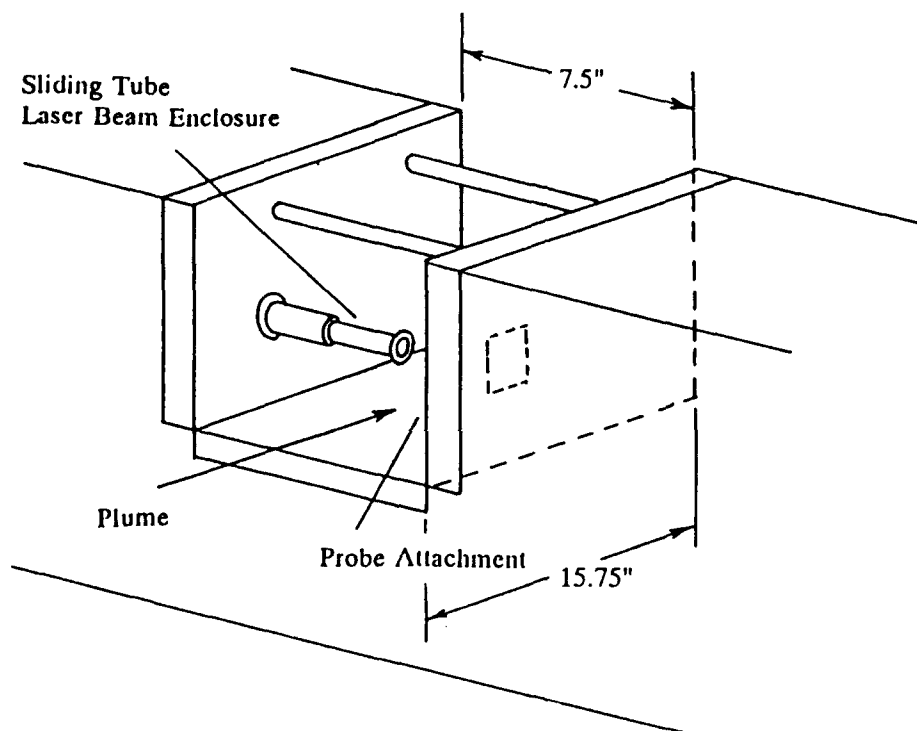
APPENDIX A
DESIGN DRAWINGS



SCHEMATIC OF INITIAL PROBE CONFIGURATION



COLLECTION PROBE EXTENSION/DIFFUSER



SCHEMATIC OF MALVERN
ENCLOSURE/PROBE SUPPORT

APPENDIX B.

TABLES

TABLE I. VARIATION BETWEEN GAS AND SOLID PRODUCTS IN TWO PHASE FLOW LOSS [Ref. 1, p 376].

	Gas	Al ₂ O ₃ Particulates		
		1 μ m	3 μ m	5 μ m
U, ft/s	8700	8600	8400	8200
T, K°	2300	2400	2600	2800
Particle mass fraction	----	0.14	0.14	0.14
Exit pressure, atm	8.50	----	----	----
Ambient pressure, atm	0.85	----	----	----
Exit radius, ft	0.25	----	----	----

TABLE II. CHARACTERISTICS OF SOLID PROPELLANT DD5 (AFAL) AND SHUTTLE PROPELLANT (Morton Thiokol)

DD5		SHUTTLE PROPELLANT	
Aluminum	4.69%	Aluminum	16.0%
AP	70.31%	AP	70.0%
GAP	14.67%	HTPB	13.8%
HDI	.845%	FE ₂ O ₃	0.2%
N100	.845%		
TEGON	8.49%		
TEPANOL	.15%		

Burning rate exponent

n=.442

r₂₅₀=.438 in/sec

r₅₀₀=.673 in/sec

Burning rate exponent

n=.350

r₆₂₅=.37 in/sec

TABLE III. LABTECH NOTEBOOK CHANNEL ASSIGNMENTS

CH #	INTERFACE DEVICE	CHANNEL NAME	CHANNEL TYPE	FILE NAME
1			TIME	
2	1:DASH-1	PRESSURE	ANALOG INPUT	1KEL (DATE) .PRN
3		1	TIME	
4		2	CALCULATED	
5		3	CALCULATED	
6		4	CALCULATED	
7		5	CALCULATED	
8	0:PIO-12	PURGE	DIGITAL OUTPUT	2KEL (DATE) .PRN
9	0:PIO-12	BACK	DIGITAL OUTPUT	3KEL (DATE) .PRN
10	0:PIO-12	IGNITION	DIGITAL OUTPUT	4KEL (DATE) .PRN
11	0:PIO-12	SCANNER	DIGITAL OUTPUT	5KEL (DATE) .PRN
12	0:PIO-12	DEFLECTOR	DIGITAL OUTPUT	6KEL (DATE) .PRN
13	0:PIO-12	MALVERN	DIGITAL OUTPUT	7KEL (DATE) .PRN

**TABLE IV. LINEAR REGRESSION OF
TRANSDUCER CALIBRATION**

VOLTS	PRESSURE
0.045	0
1.142	100
2.215	200
3.300	300
4.367	400
5.438	500
6.523	600
7.603	700
8.654	800

Regression Output:

Constant	-5.568
Std Err of Y Est	0.971
R Squared	1.0
No. of Observations	9
Degrees of Freedom	7
X Coefficient(s)	92.912
Std Err of Coef.	0.116

TABLE V. MOTOR AND PROBE RESULTS

TEST DATE	P _c PSIA	MEASUREMENT LOCATION ¹	% Al	SEM PARTICLE COUNT
2-14	275	22 C	16	1298
2-26	350	16 C	4.69	1232
2-28	350	35 C	4.69	543
3-08	350	35 R	4.69	6427
3-12	350	35 R	4.69	3495
3-14	300	25 C	4.69	3359

¹ Distance from nozzle exit in exit jet diameters

C= centerline, R= off centerline

TABLE VI. MALVERN AND SEM PARTICLE SIZE DATA FROM VOLUME AND NUMBER DISTRIBUTIONS

TEST DATE	SIZE RANGE FROM NUMBER DISTRIBUTION		SIZE RANGE FROM MALVERN VOLUME DISTRIBUTION
	MALVERN	SEM	
2-14	0.2 - 5.8	0.16 - 7.0 (10.3, 18.3) ¹	0.2 - 7.0
2-26	0.2 - 3.3	0.16 - 4.0	0.2 - 4.8
2-28	0.2 - 10.3	0.13 - 8.5	0.6 - 12.4
3-08	0.2 - 7.0	0.13 - 10.3 (22, 50)	0.2 - 102.0
3-12	0.2 - 4.0	0.13 - 7.0 (18.3)	0.7 - 5.8 (84) ²
3-14	0.2 - 8.5	0.13 - 10.3	0.2 - 22.0 (84)

¹ Single particle sizes outside of reported range

² Indicates maximum size, but probably the result of beam steering

APPENDIX C

FIGURES

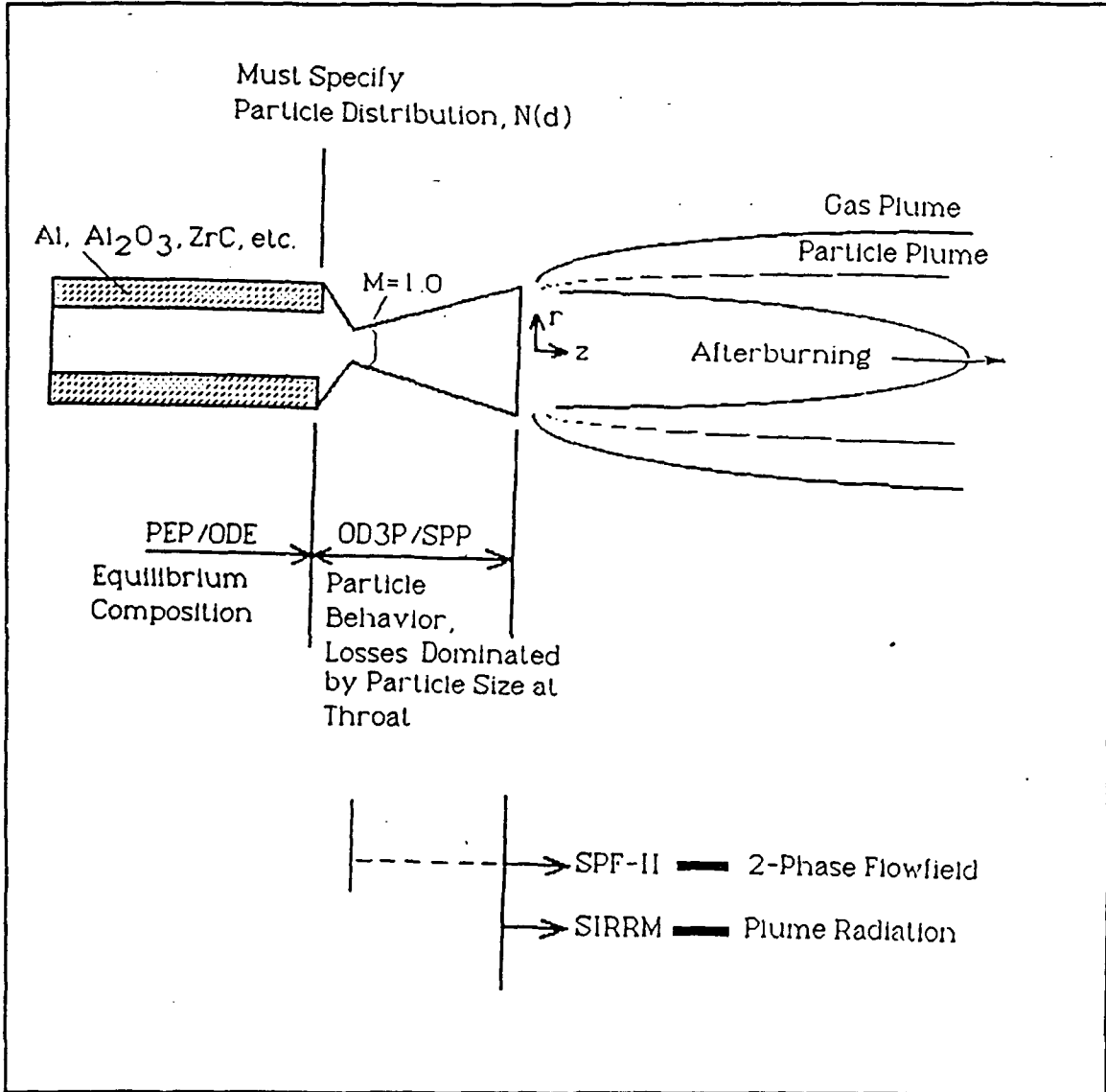


Figure 1.1. Sequence of Computer Codes in the Calculation of Rocket Motor Performance and Plume Signature.

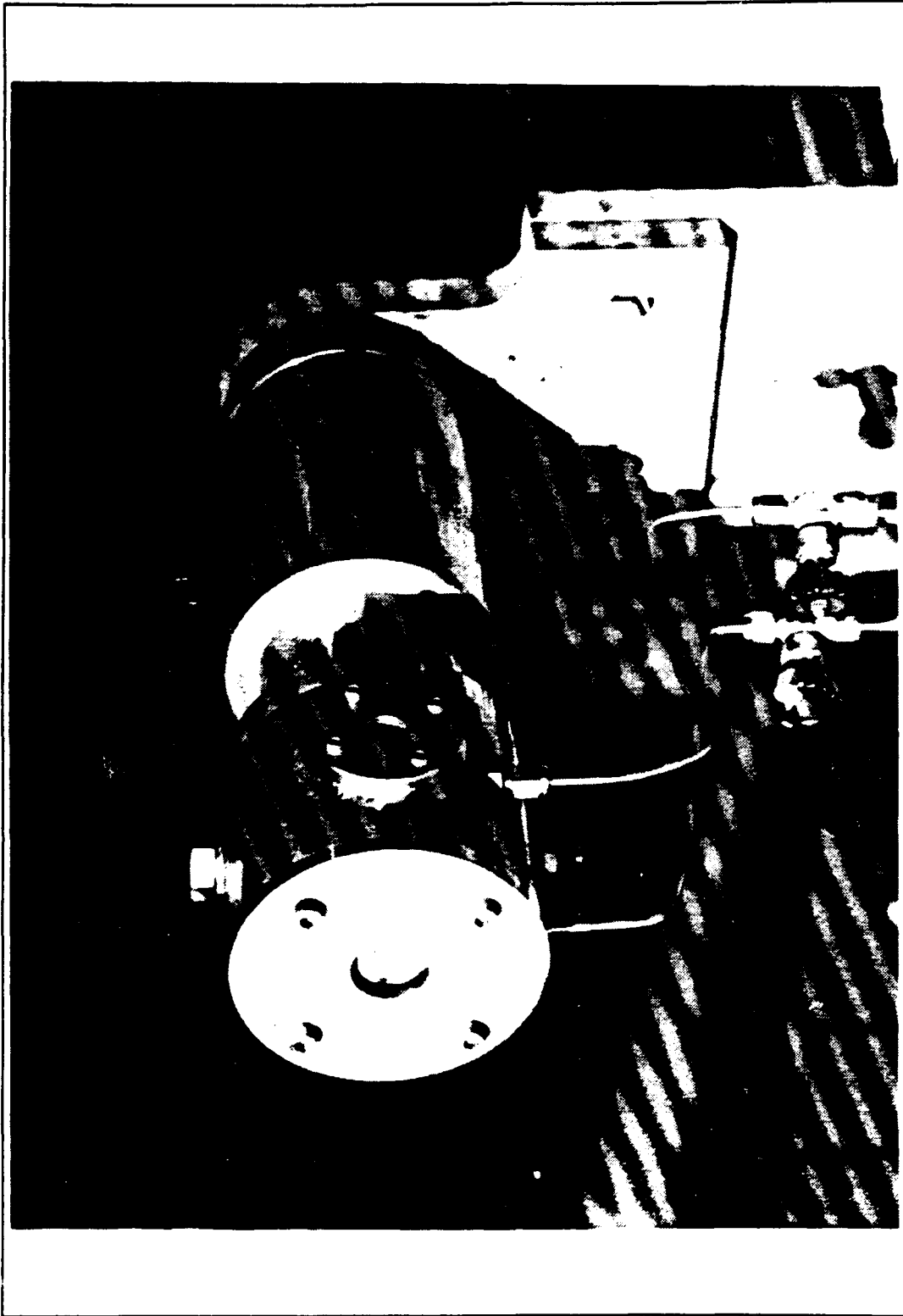


Figure 2.1. Three Dimensional Subscale Motor. [Ref. 8]

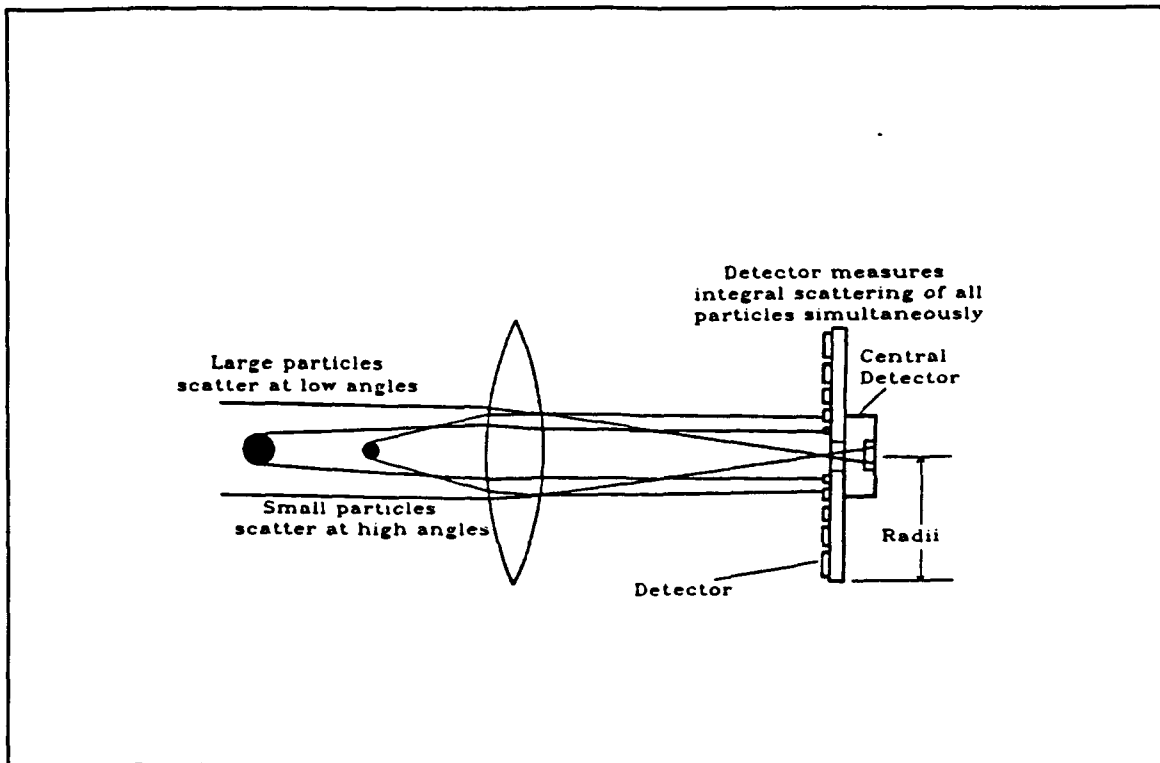


Figure 2.2. Malvern Light Scattering Principle
 [Ref. 11, p. 1-16].

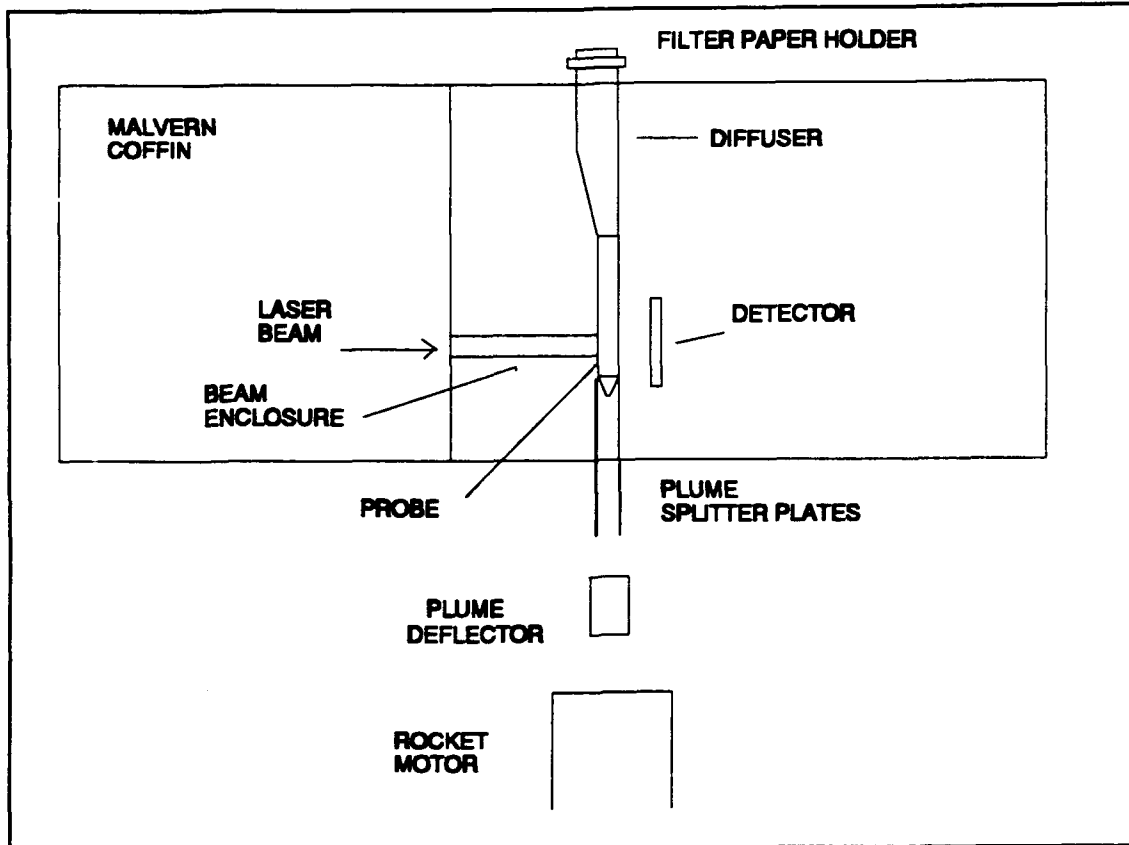


Figure 2.3. Malvern Enclosure and Plume Splitter.

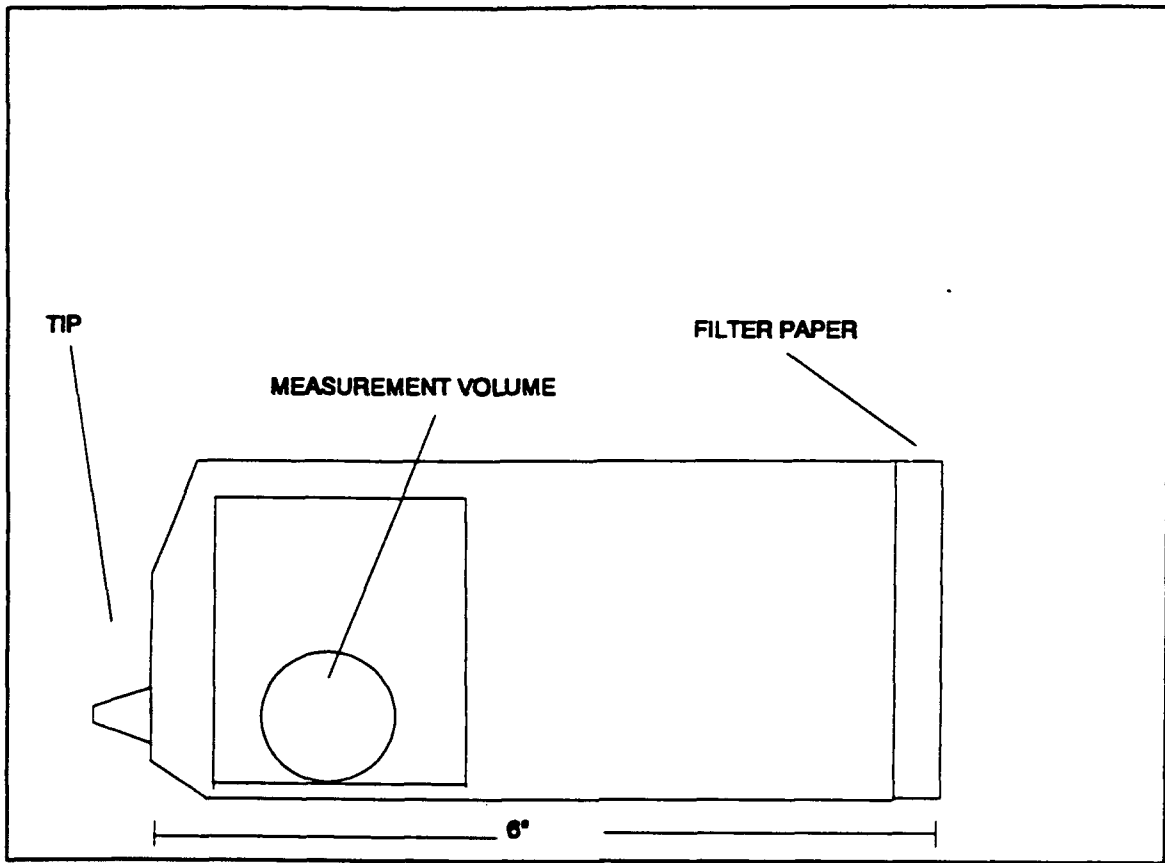


Figure 2.4. Probe Before Modification.

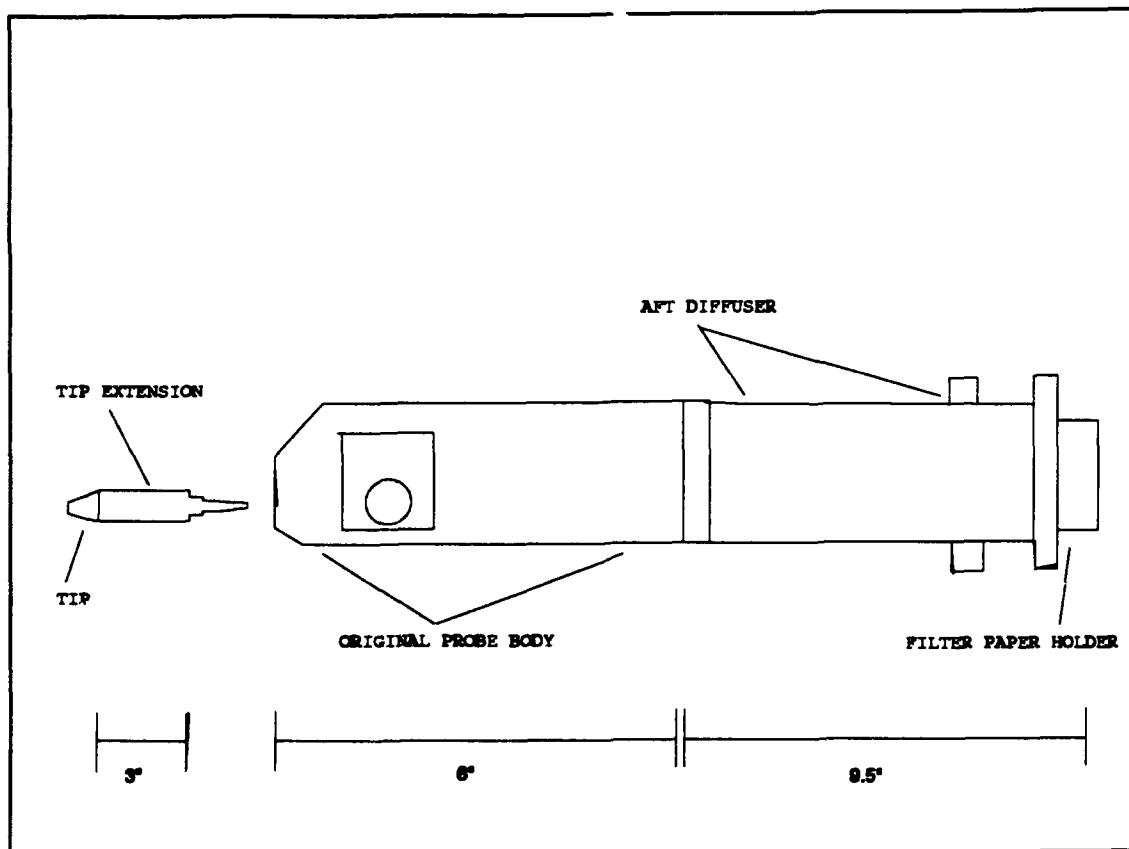


Figure 2.5. Probe After Modification.

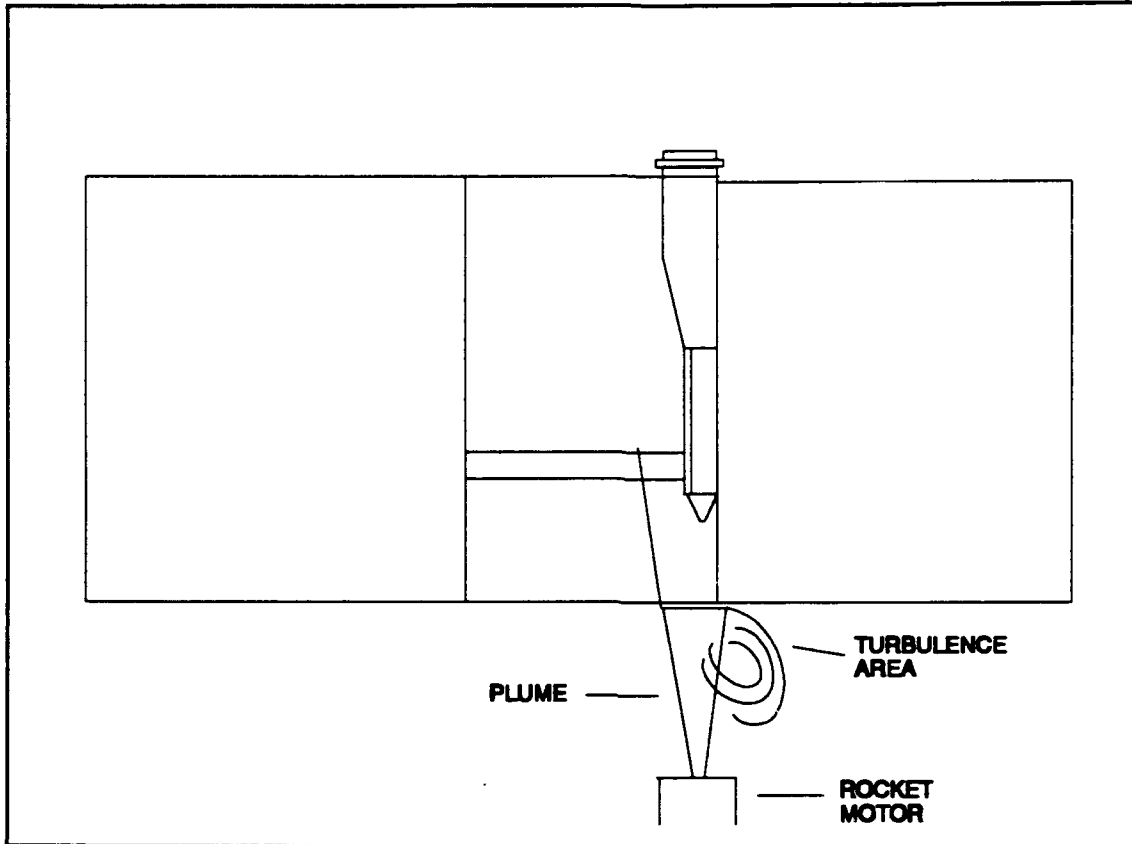


Figure 2.6. Malvern Enclosure Interaction With Plume.

4.69% ALUMINUM PROPELLANT

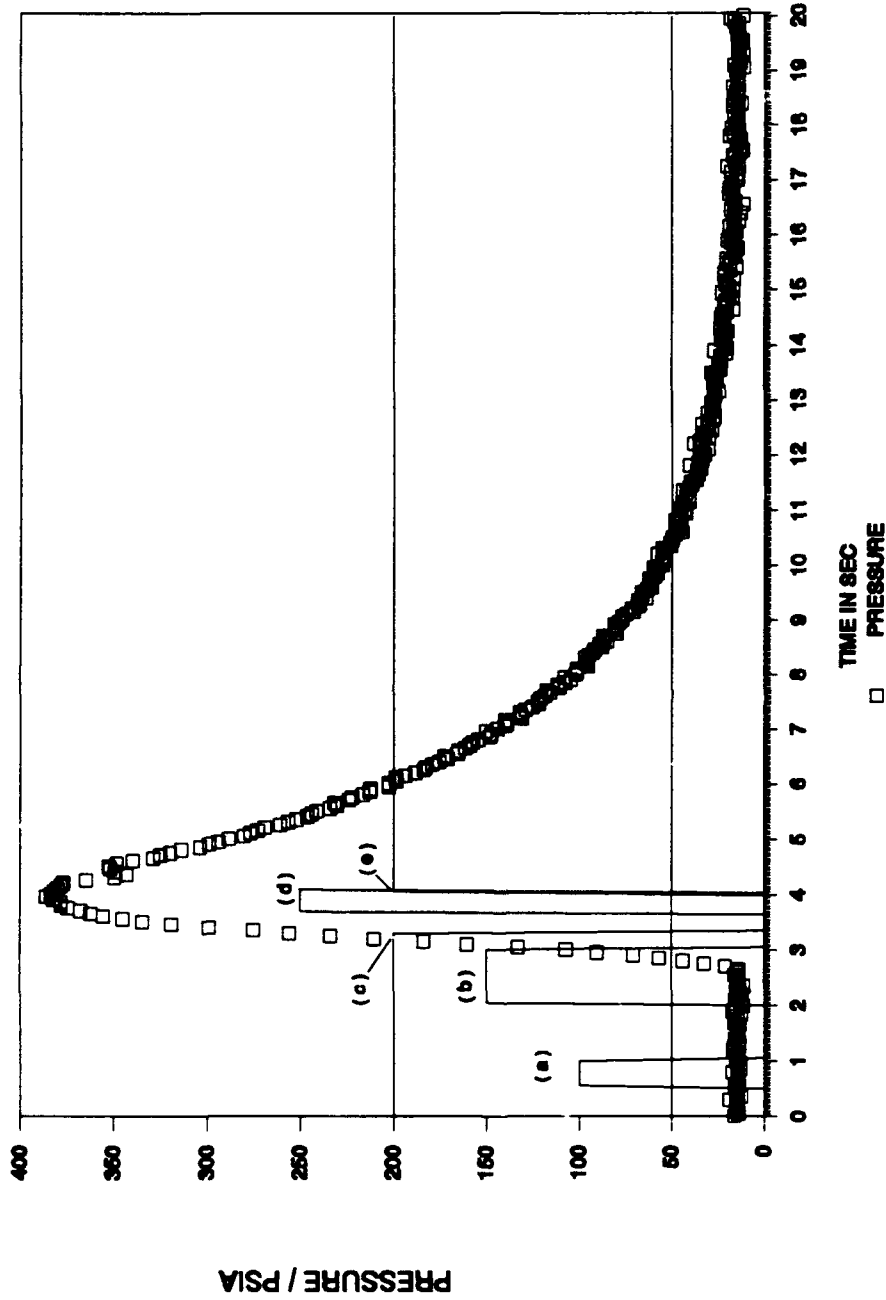


Figure 2.7. Labtech Notebook Firing/Data Control. The Sequence of Triggering Which Follow Purge at t=0 are (a) Measure Background, (b) Ignition, (c) Deflector Down, (d) Measure Sample, and (e) Deflector Up.

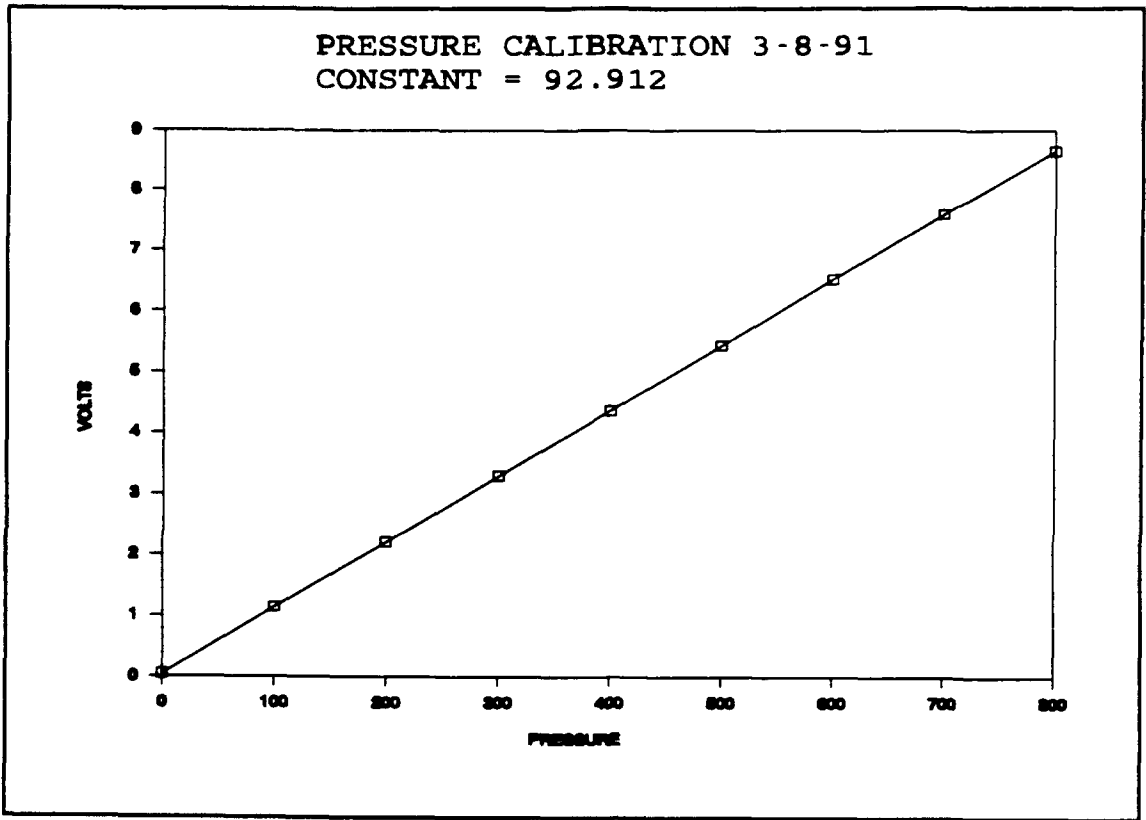
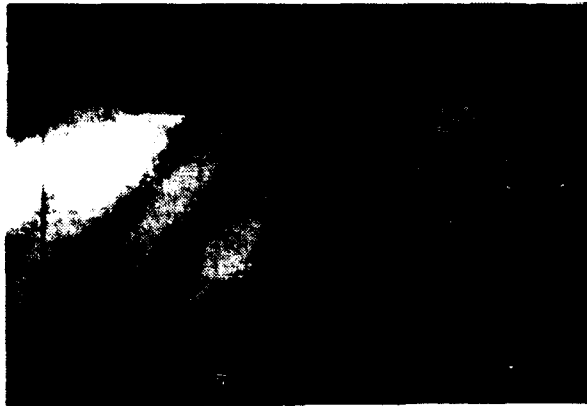


Figure 3.1. Pressure Calibration of Transducer During Pre-fire Check.



(a) NO FLOW
CONDITION



(b) OVEREXPANDED
EXHAUST FLOW $P_e = 11 \text{ psia}$
DETACHED CONICAL SHOCK
ON PROBE TIP

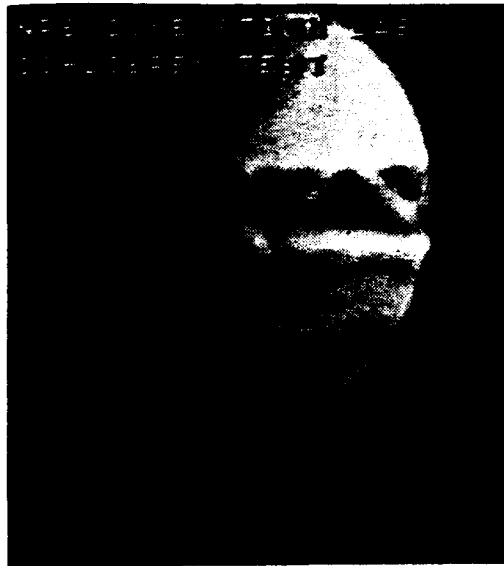


(c) UNDEREXPANDED
EXHAUST FLOW $P_e = 21 \text{ psia}$
SHOCK SWALLOWED AT
PROBE TIP

Figure 4.1. Schlieren of Supersonic Nozzle Exhaust Flow Into Probe Tip.



(a) NO FLOW CONDITIONS



(b) UNDEREXPANDED EXHAUST FLOW
Pe= 21 psia

Figure 4.2 Schlieren of Probe Flow with 8° Half-Angle Wedge Located within the Measurement Volume.

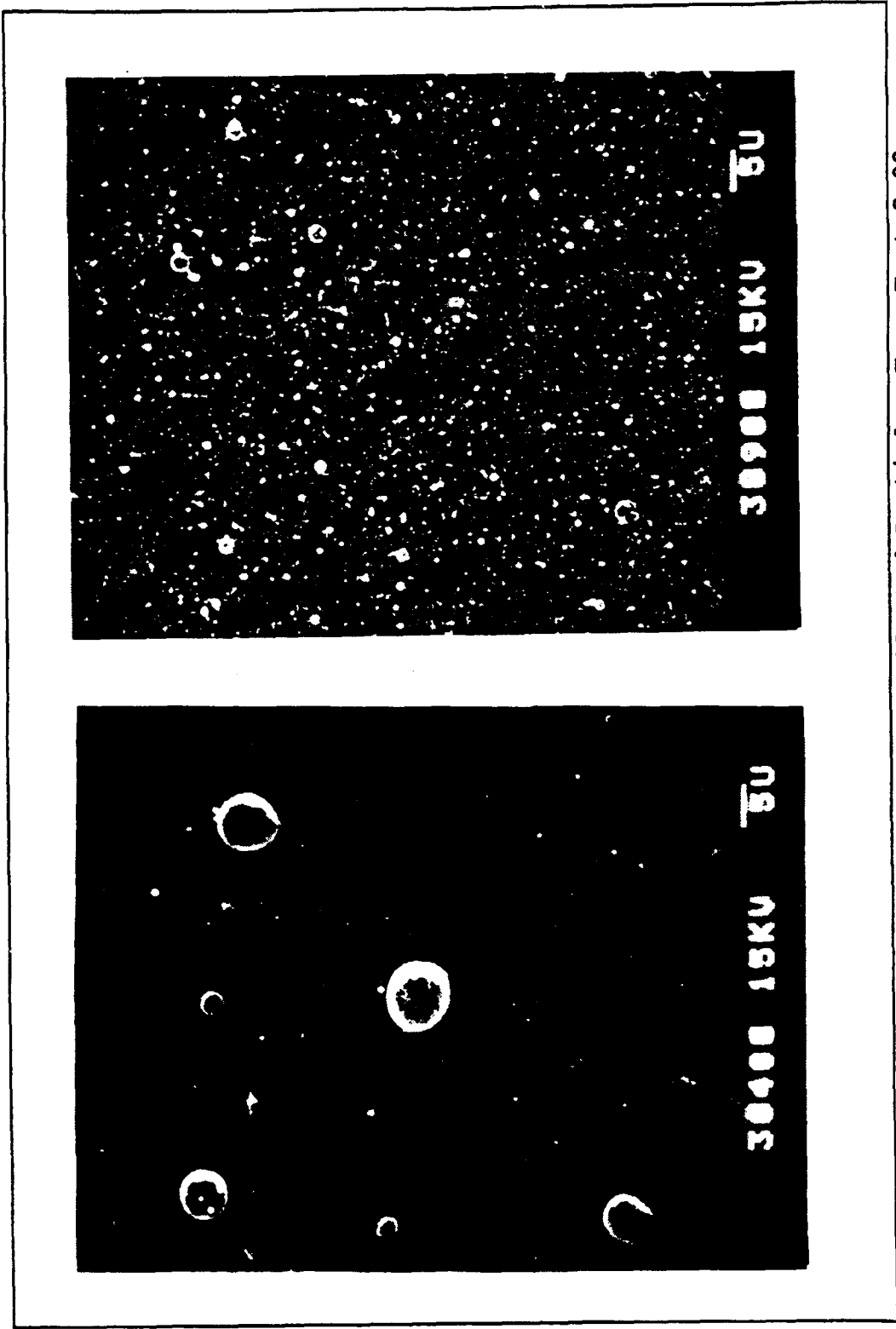


Figure 4.3. SEM Photographs of Collected Particles From Test 3-08.

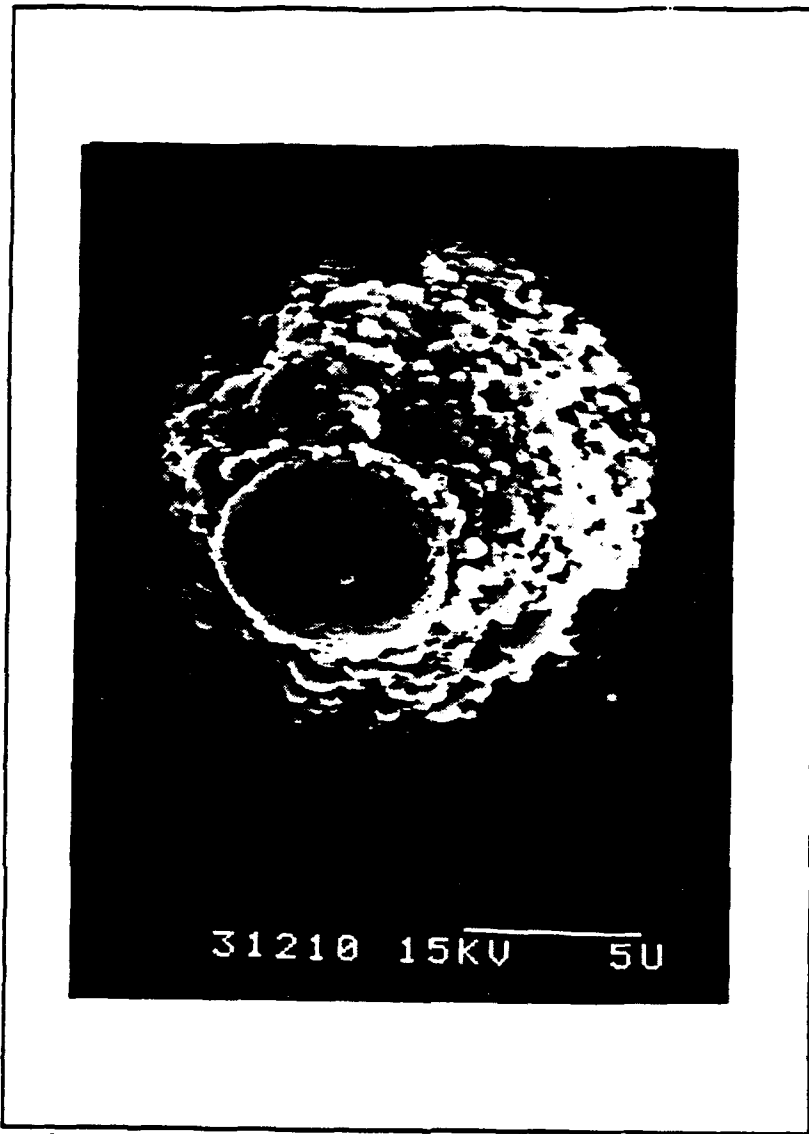


Figure 4.4. Example of Large Agglomerate from Test 3-12.

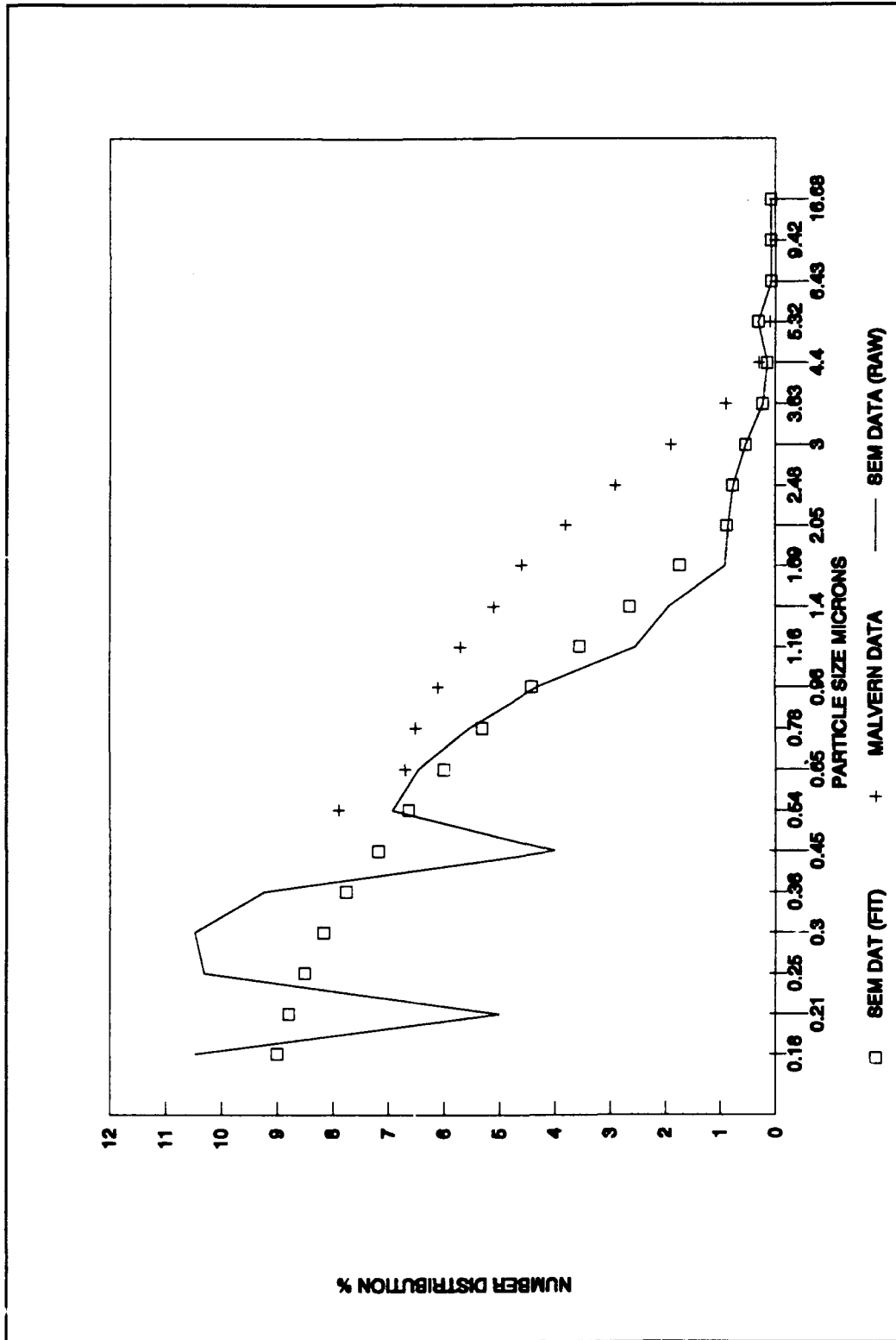


Figure 4.5. Number Distributions for Test 2-14 Obtained from SEM Photographs of Collected Particles and from Measurements Using the Malvern Mastersizer.

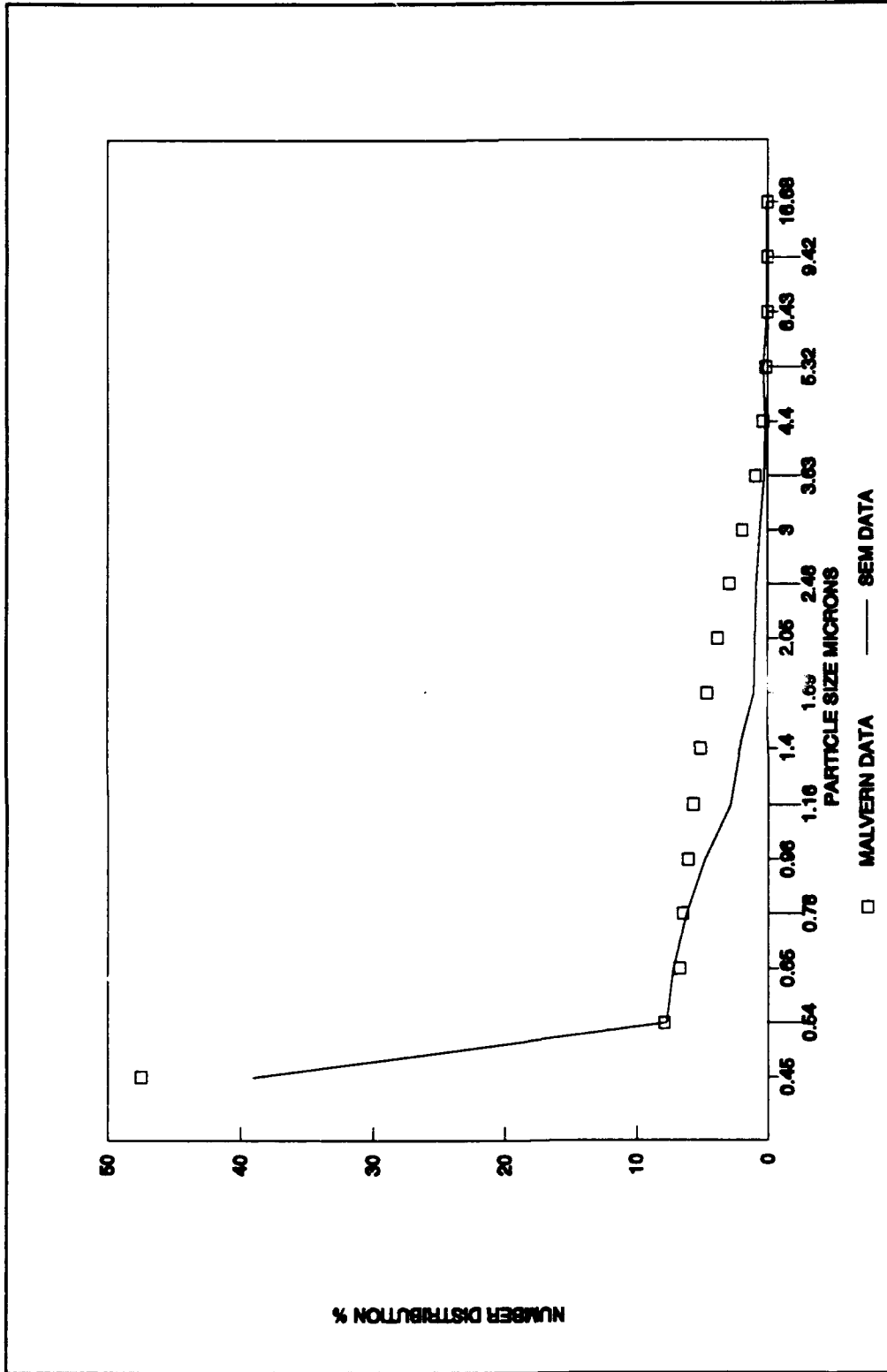


Figure 4.6. Number Distributions for Test 2-14 Obtained from Photographs of Collected Particles and from In Situ Measurements Using the Malvern Mastersizer, for Particles in Common Measurement Range.

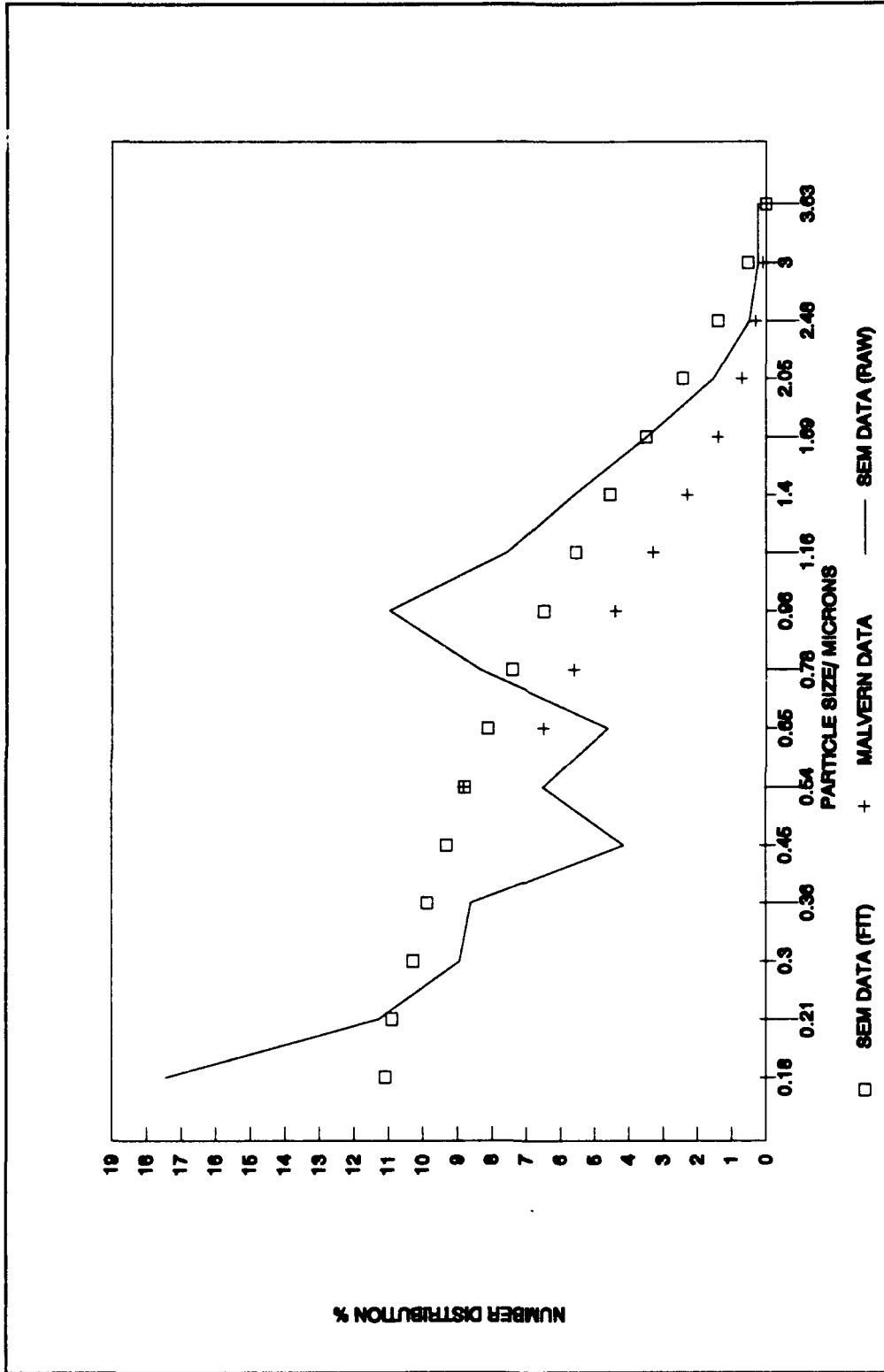


Figure 4.7. Number Distributions for Test 2-26 Obtained from SEM Photographs of Collected Particles and from Measurements Using the Malvern Mastersizer.

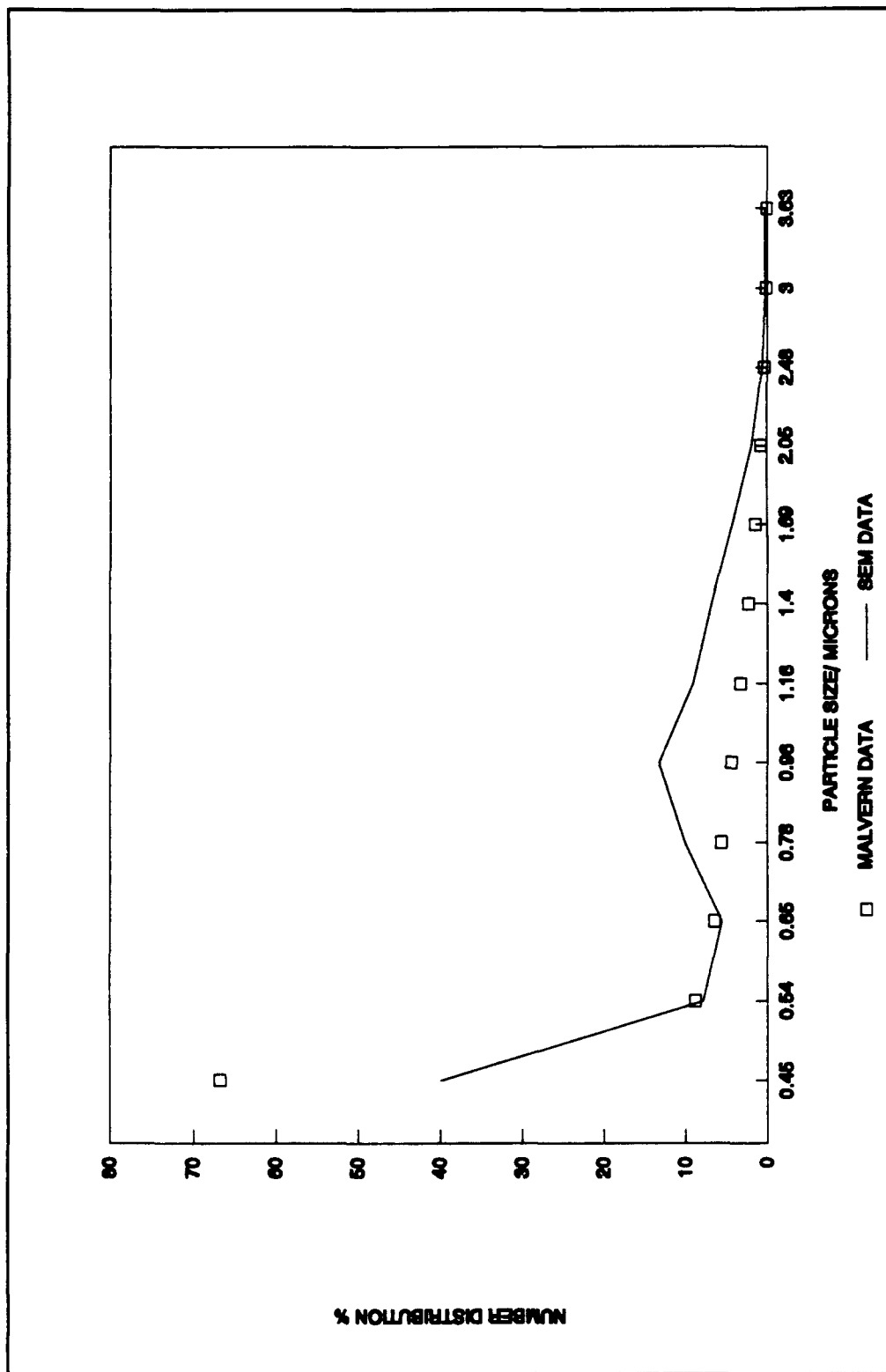


Figure 4.8. Number Distributions for Test 2-26 Obtained from Photographs of Collected Particles and from In Situ Measurements Using the Malvern Mastersizer, for Particles in Common Measurement Range.

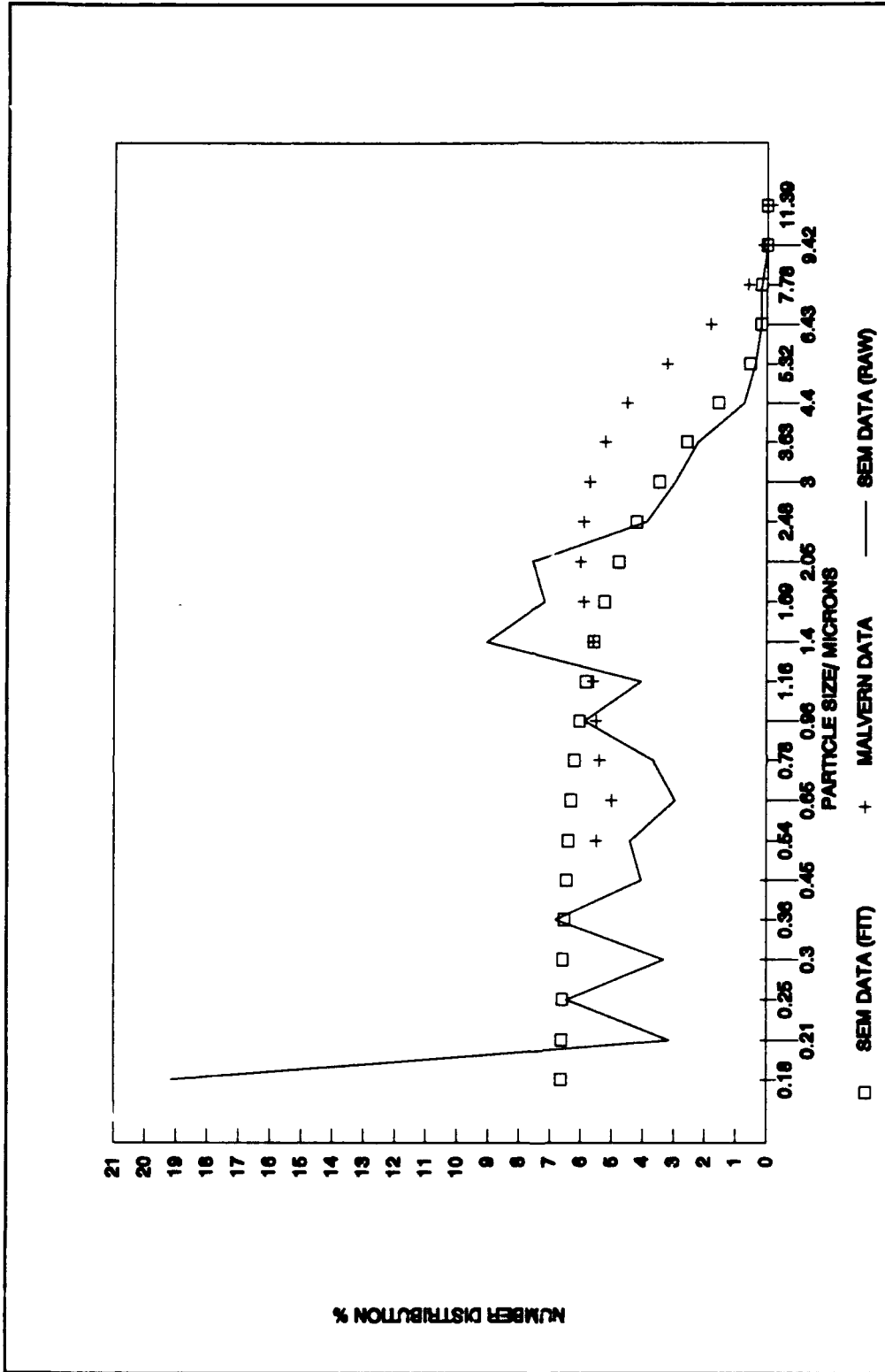


Figure 4.9. Number Distributions for Test 2-28 Obtained from SEM Photographs of Collected Particles and from Measurements Using the Malvern Mastersizer.

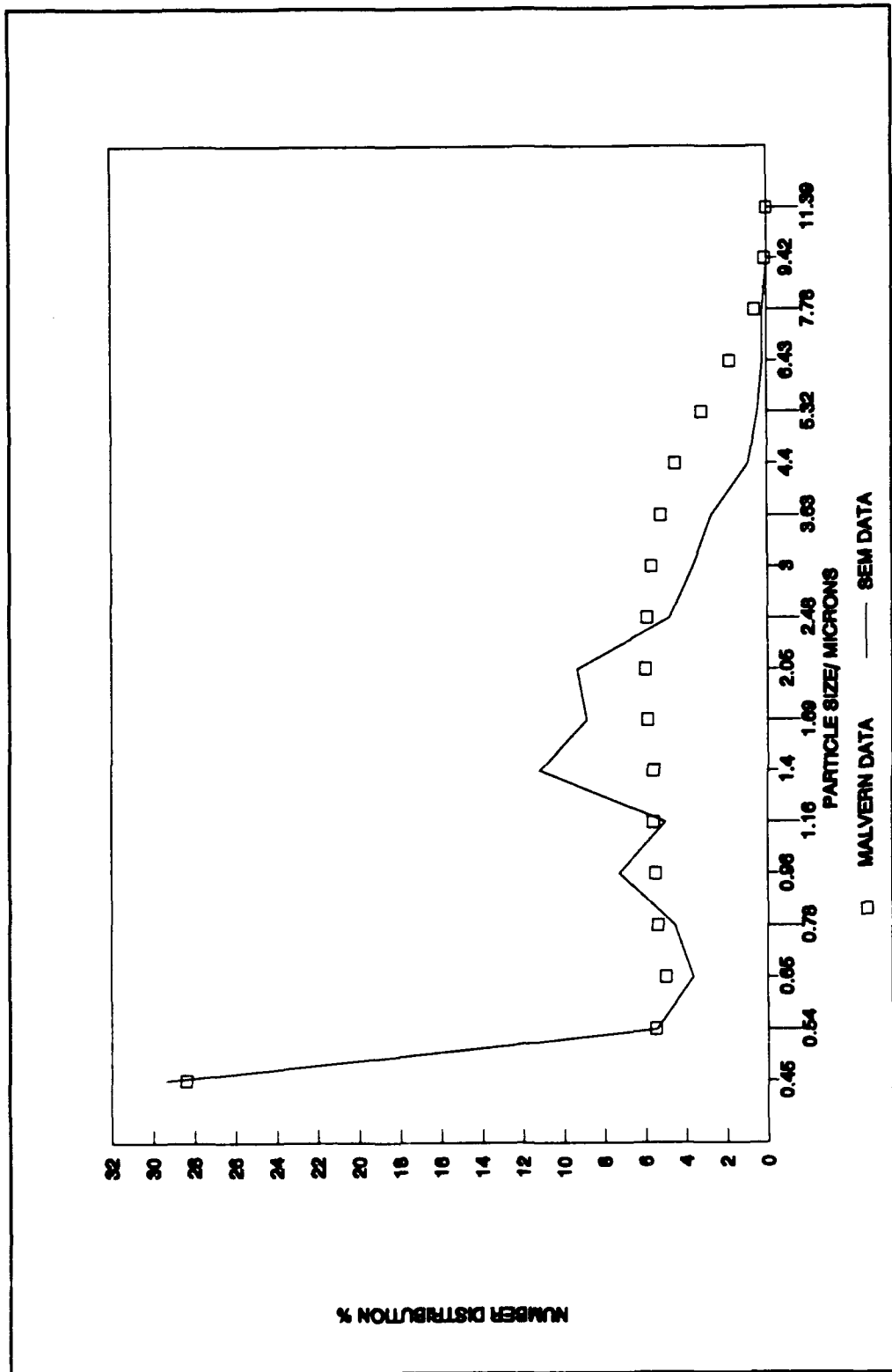


Figure 4.10. Number Distributions for Test 2-28 Obtained from Photographs of Collected Particles and from In Situ Measurements Using the Malvern Mastersizer, for Particles in Common Measurement Range.

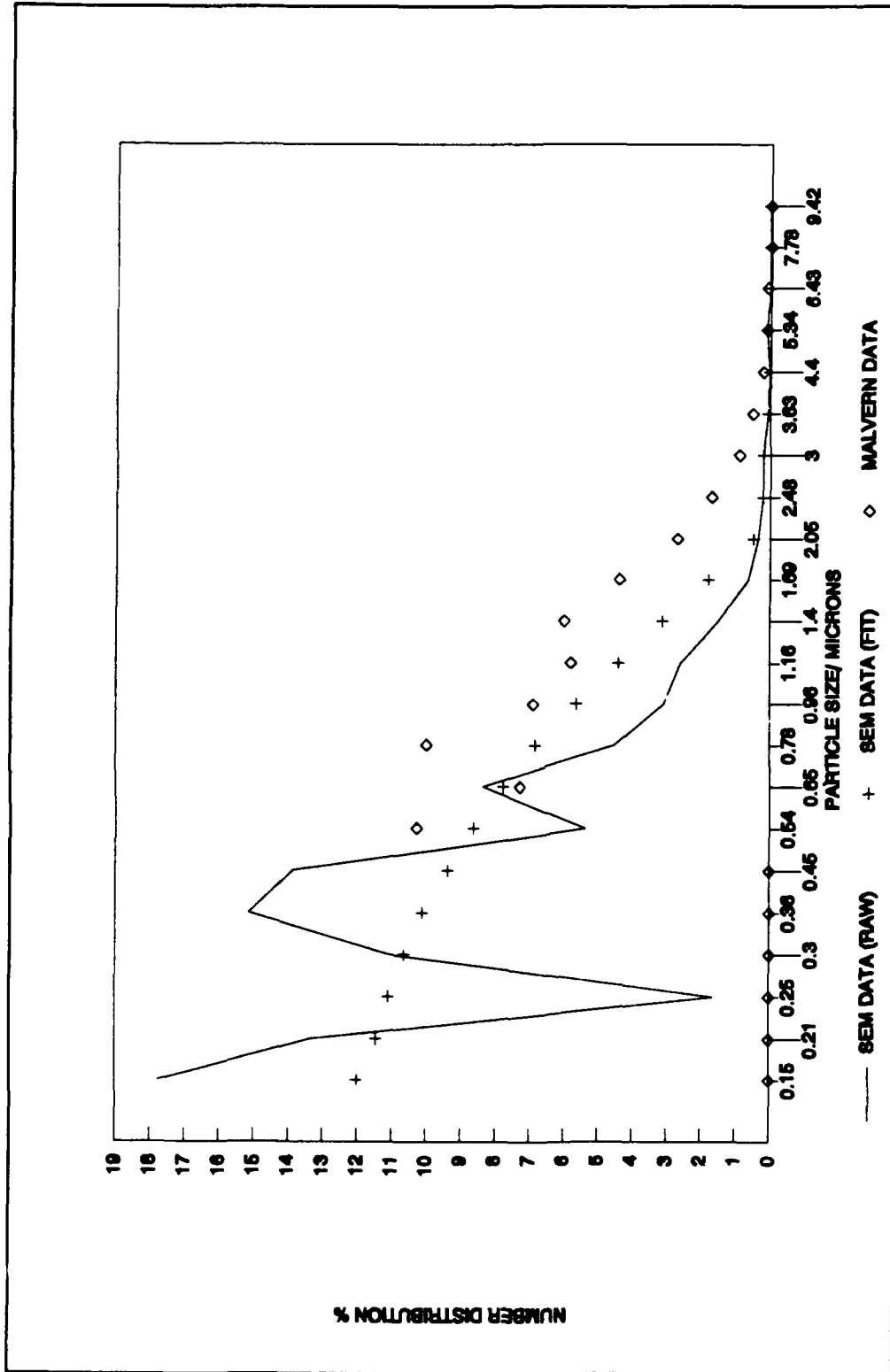


Figure 4.11. Number Distributions for Test 3-08 Obtained from SEM Photographs of Collected Particles and from Measurements Using the Malvern Mastersizer.

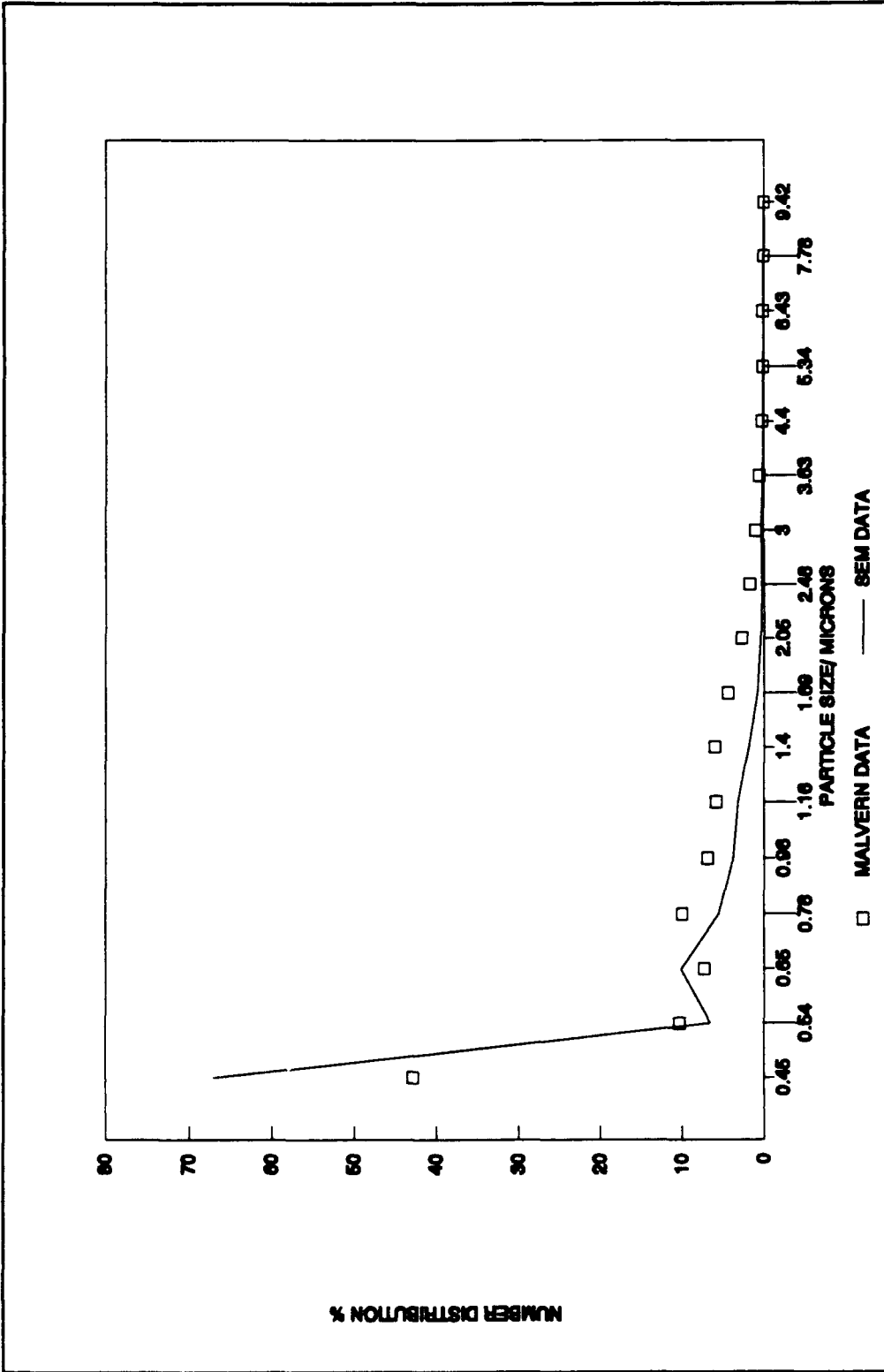


Figure 4.12. Number Distributions for Test 3-08 Obtained from Photographs of Collected Particles and from In Situ Measurements Using the Malvern Mastersizer, for Particles in Common Measurement Range.

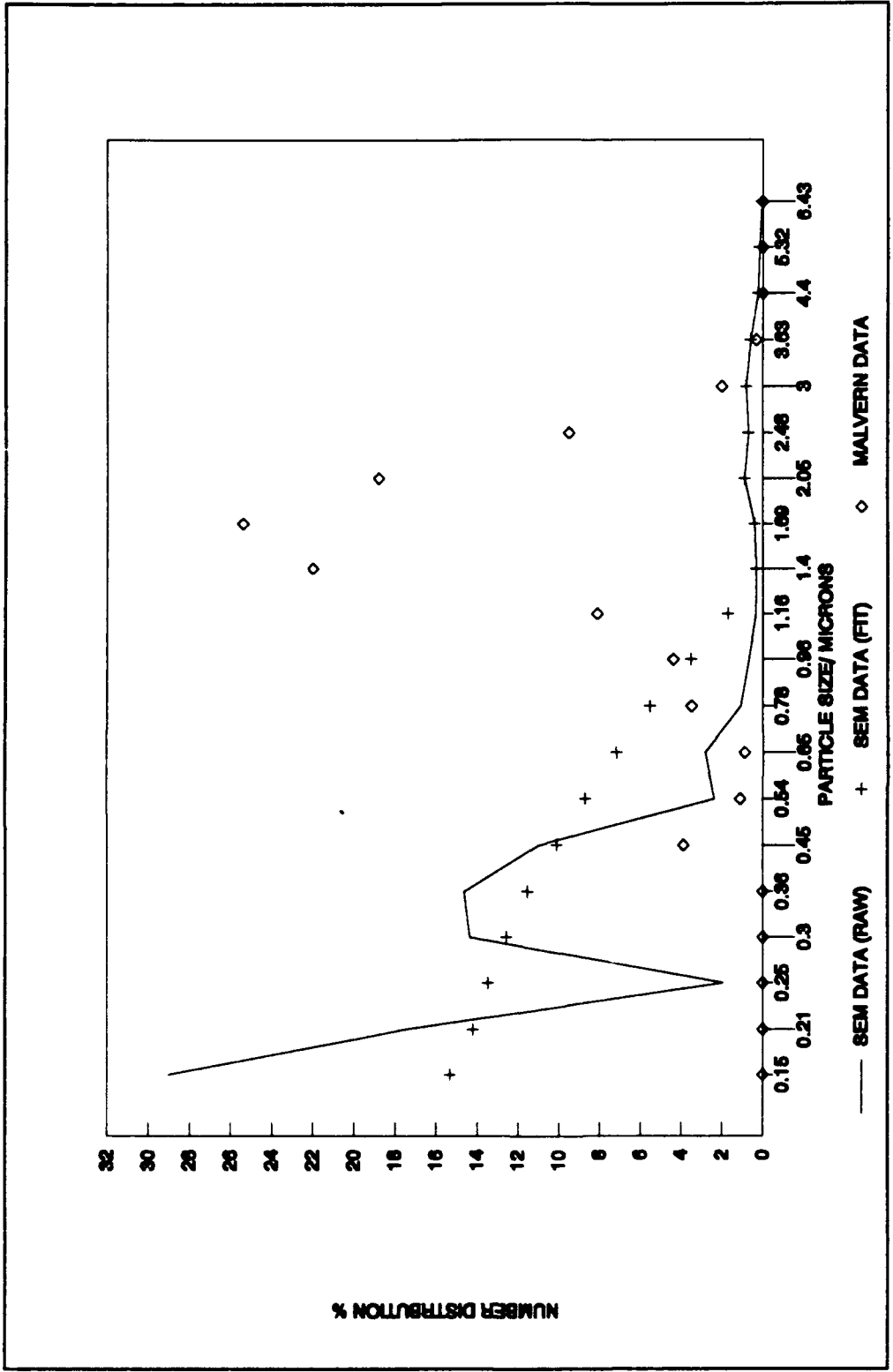


Figure 4.13. Number Distributions for Test 3-12 Obtained from SEM Photographs of Collected Particles and from Measurements Using the Malvern Mastersizer.

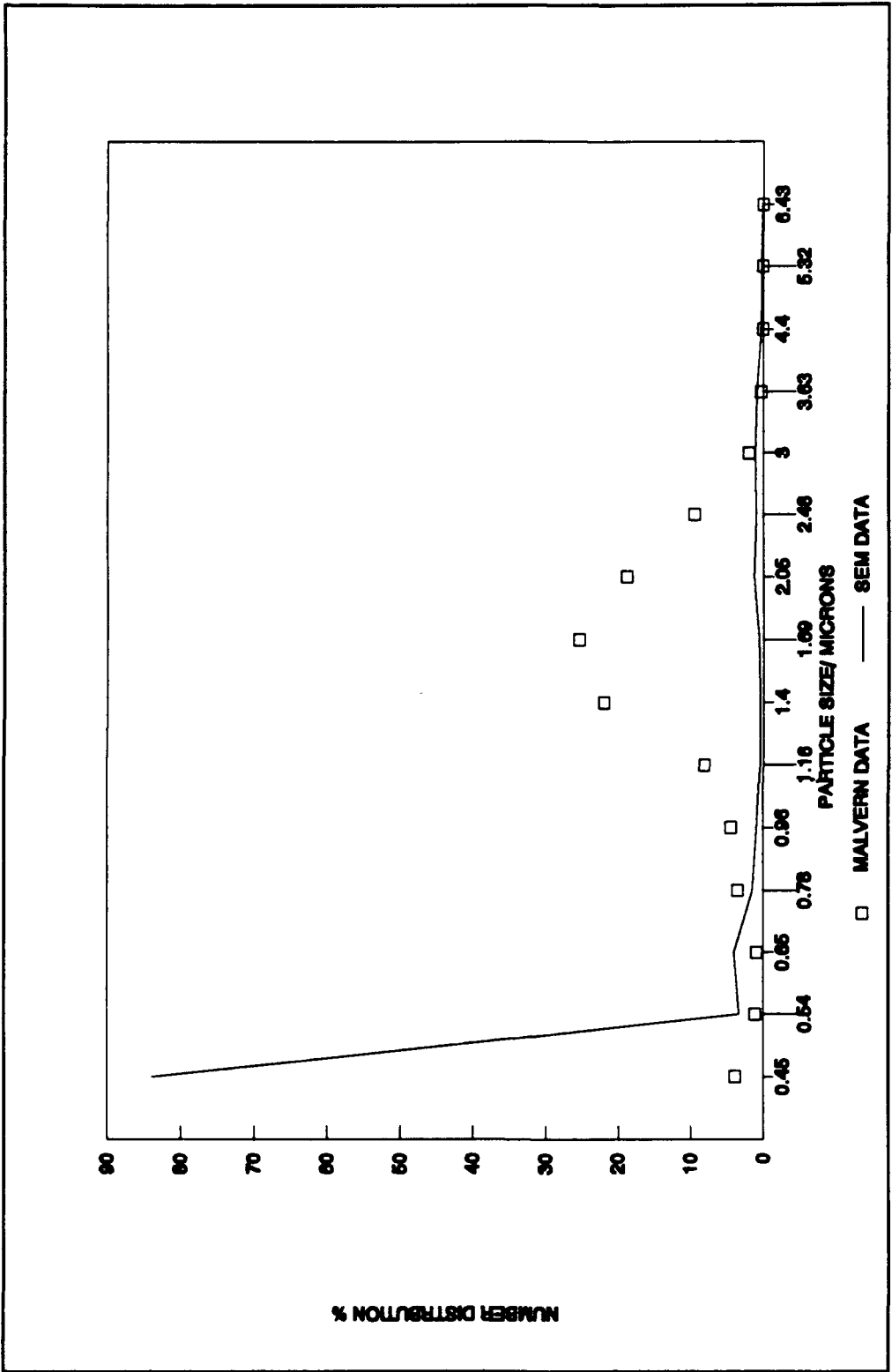


Figure 4.14. Number Distributions for Test 3-12 Obtained from Photographs of Collected Particles and from In Situ Measurements Using the Malvern Mastersizer, for Particles in Common Measurement Range.

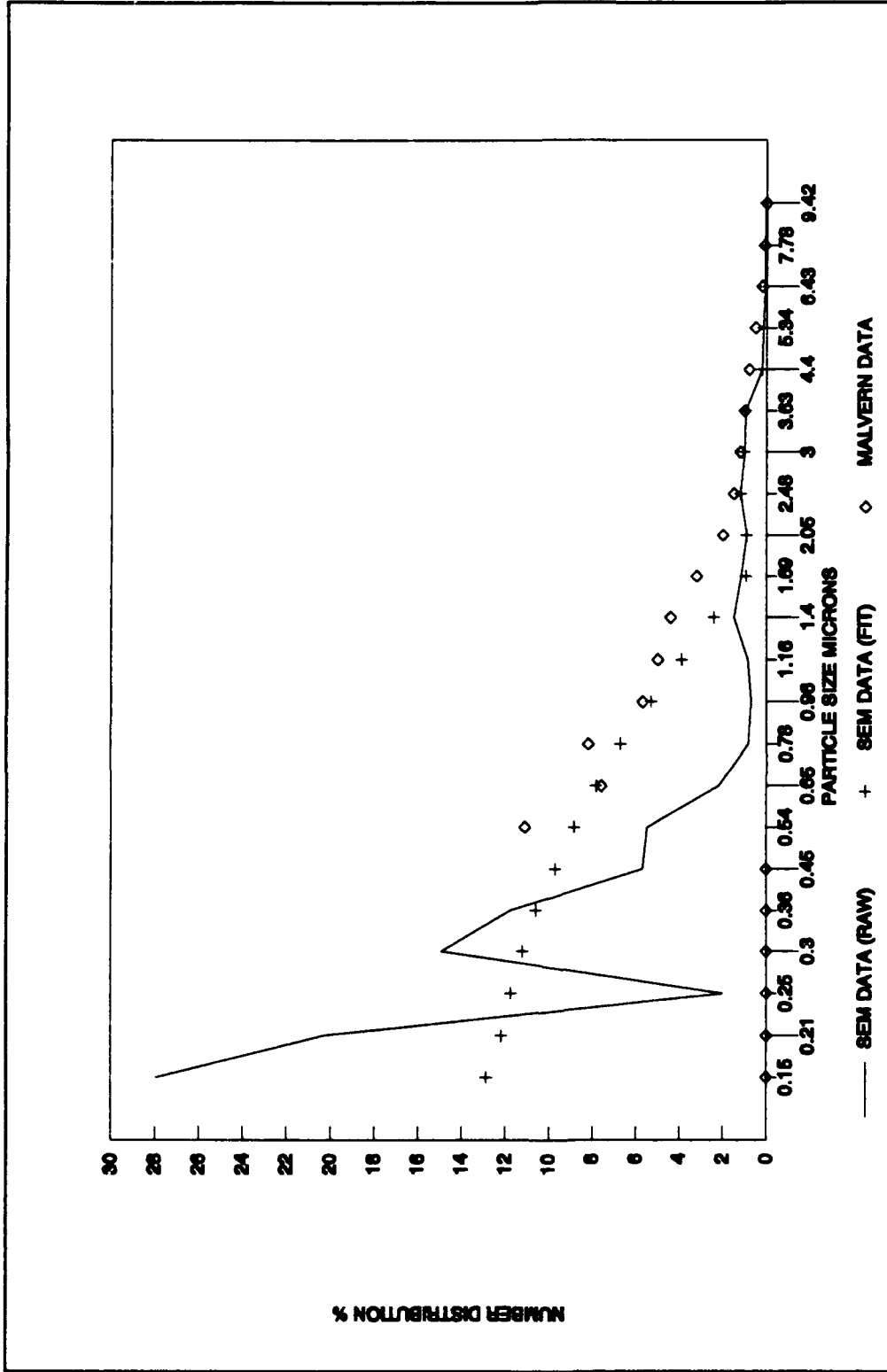


Figure 4.15. Number Distributions for Test 3-14 Obtained from SEM Photographs of Collected Particles and from Measurements Using the Malvern Mastersizer.

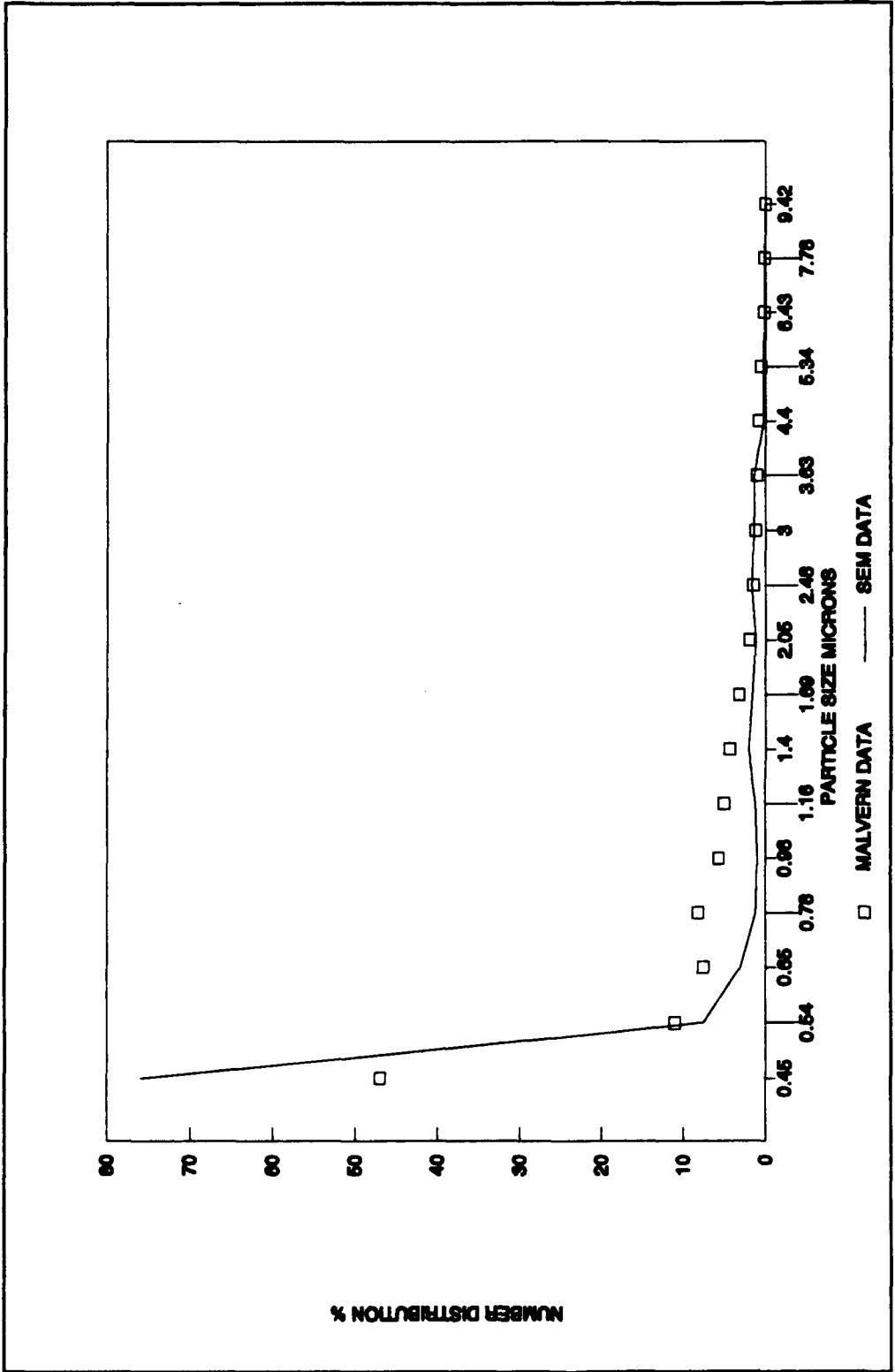


Figure 4.16. Number Distributions for Test 3-14 Obtained from Photographs of Collected Particles and from In Situ Measurements Using the Malvern Mastersizer, for Particles in Common Measurement Range.

APPENDIX D

MICROPEP OUTPUT

1

**** NEWPEP - Feb. 1990 ****
* 01/25/91 * DH ** DENS **** COMPOSITION *****

* lyle

ALUMINUM (PURE CRYSTALLINE)	0	0.09760	1AL			
AMMONIUM PERCHLORATE (AP)	-602	0.07040	1CL	4H	1N	4O
FERRIC OXIDE HEMATITE	-1235	0.18480	2FE	3O		
HTPB/CURATIVE (JOS)	-5	0.03290	656C	978H	5N	13O

INGREDIENT WEIGHTS (IN ORDER) AND TOTAL WEIGHT (LAST ITEM IN LIST)

16.0000	70.0000	0.2000	13.8000	100.0000
---------	---------	--------	---------	----------

THE PROPELLANT DENSITY IS 0.06334 LB/CU-IN OR 1.7532 GM/CC

NUMBER OF GRAM ATOMS OF EACH ELEMENT PRESENT IN INGREDIENTS

3.859172 H	0.990126 C	0.603307 N	2.406418 O
0.593032 AL	0.595760 CL	0.002505 FE	

*****CHAMBER RESULTS FOLLOW*****

T(K)	T(F)	P(ATM)	P(PSI)	ENTHALPY	ENTROPY	CP/CV	SGAMMA	RT/V	TCRE
3282.	5448.	20.41	300.00	-42.46	2.7-84	1.1809	1.1352	5.584	

DAMPED AND UNDAMPED SPEED OF SOUND= 2981.126 AND 3560.087 FT/SEC

SPECIFIC HEAT (MOLAR) OF GAS AND TOTAL=	9.451	12.051
NUMBER MOLS GAS AND CONDENSED=	3.6546	0.2798

1.10101 H2	0.93748 CO	0.51159 HCl	0.47937 H2O
0.30070 N2	0.27983 Al2O3*	0.15515 H	0.05255 CO2
0.04817 Cl	0.02805 HO	0.01840 AlCl	0.00561 AlOCl
4.10E-03 AlCl2	2.32E-03 O	1.90E-03 AlHO2	1.82E-03 NO
1.44E-03 AlHO	1.17E-03 FeCl2	1.16E-03 Fe	7.36E-04 AlO
4.37E-04 Al	4.00E-04 O2	3.87E-04 AlCl3	1.36E-04 Al2O
8.57E-05 FeCl	6.37E-05 FeO	5.84E-05 Cl2	5.46E-05 AlH
4.75E-05 CHO	2.12E-05 NH3	2.03E-05 COCl	1.86E-05 OCl
1.71E-05 FeH2O2	1.70E-05 N	1.51E-05 HOCl	1.38E-05 Al2O2
1.22E-05 CNH	1.06E-05 NH2	6.51E-06 NH	5.33E-06 AlO2
3.23E-06 CH2O	3.06E-06 HO2	2.13E-06 NHO	1.18E-06 AlHO
8.92E-07 CNHO	5.58E-07 FeCl3	2.73E-07 CN	

THE MOLECULAR WEIGHT OF THE MIXTURE IS 25.417

TOTAL HEAT CONTENT (298 REF)	=1345.926 CAL/GM
SENSIBLE HEAT CONTENT (298 REF)	=1258.734 CAL/GM

*****EXHAUST RESULTS FOLLOW*****

T(K)	T(F)	P(ATM)	P(PSI)	ENTHALPY	ENTROPY	CP/CV	SGAMMA	RT/V	TCRE
2328.	3731.	1.00	14.70	-102.53	237.84	1.1792	1.1595	0.283	

DAMPED AND UNDAMPED SPEED OF SOUND= 2434.872 AND 2947.180 FT/SEC

SPECIFIC HEAT (MOLAR) OF GAS AND TOTAL=	9.225	12.068
NUMBER MOLS GAS AND CONDENSED=	3.5358	0.2962

1.16528 H2	0.92527 CO	0.58217 HCl	0.46104 H2O
0.30162 N2	0.29620 Al2O3*	0.06484 CO2	0.02274 H
8.13E-03 Cl	2.31E-03 FeCl2	1.54E-03 HO	2.89E-04 AlCl

1.72E-04 Fe	1.30E-04 AlOCl	1.15E-04 AlCl2	5.01E-05 AlCl3
4.30E-05 NO	2.07E-05 AlHO2	2.00E-05 O	1.29E-05 AlHO
9.64E-06 FeCl	3.97E-06 Cl2	3.30E-06 O2	3.04E-06 FeH2O2
2.68E-06 FeO	2.54E-06 NH3	1.08E-06 CHO	6.68E-07 CNH
5.84E-07 AlO	5.43E-07 COCl	3.56E-07 Al	3.53E-07 FeCl3
2.79E-07 HOCl			

THE MOLECULAR WEIGHT OF THE MIXTURE IS 26.096

TOTAL HEAT CONTENT (298 REF) = 859.631 CAL/GM
 SENSIBLE HEAT CONTENT (298 REF)= 808.814 CAL/GM

*****PERFORMANCE: FROZEN ON FIRST LINE, SHIFTING ON SECOND LINE*****

An exact method for determining throat conditions was used
 The frozen & shifting STATE gammas for the throat are: 1.1795 1.1368
 ISentropic EXponent shown below is the gamma for the chamber to throat PROCESS.

IMPULSE	IS	EX	T*	P*	C*	ISP*	OPT	EX	D-ISP	A*M.	EX	T	ADH
223.5	1.1815	3020.	11.87	5082.6			3.74	391.9	0.52670	2048.	500429.		
228.7	1.1361	3099.	11.78	5152.8	197.5	3.97	400.9	0.53396	2328.	575377.			

**** NEWPEP - Feb. 1990 ****

1

**** NEWPEP - Feb. 1990 ****

* lyledd5

* 02/05/91 * DH ** DENS **** COMPOSITION *****

ALUMINUM (PURE CRYSTALLINE)	0	0.09760	1AL			
AMMONIUM PERCHLORATE (AP)	-602	0.07040	1CL	4H	1N	40
GAP (ARC CALC)	309	0.04700	60C	102H	60N	210
HMDI	-717	0.03750	8C	12H	2O	2N
N-100	-280	0.04700	4C	6H	1O	1N
TEGDN (RUSS/MAY)	-645	0.04870	6C	12H	2N	8O
TEPA.NO3	-605	0.05920	8C	28H	15O	10N

INGREDIENT WEIGHTS (IN ORDER) AND TOTAL WEIGHT (LAST ITEM IN LIST)

4.6900	70.3100	14.6700	0.8450	0.8450	8.4900
0.1500	100.0000				

THE PROPELLANT DENSITY IS 0.06344 LB/CU-IN OR 1.7560 GM/CC

NUMBER OF GRAM ATOMS OF EACH ELEMENT PRESENT IN INGREDIENTS

3.694862 H	0.734962 C	1.132275 N	2.854978 O
0.173832 AL	0.598398 CL		

*****CHAMBER RESULTS FOLLOW*****

T(K)	T(F)	P(ATM)	P(PST)	ENTHALPY	ENTROPY	CP/CV	SGAMMA	RT/V	TCRE
3154.	5219.	20.41	300.00	-44.20	239.98	1.1983	1.1243	5.614	

DAMPED AND UNDAMPED SPEED OF SOUND= 3349.272 AND 3506.517 FT/SEC

SPECIFIC HEAT (MOLAR) OF GAS AND TOTAL= 10.940 11.736
NUMBER MOLS GAS AND CONDENSED= 3.6354 0.0845

1.29998 H2O	0.55543 N2	0.51457 HCl	0.40252 CO
0.33235 CO2	0.20826 H2	0.11375 HO	0.08448 Al2O3*
0.07949 Cl	0.04782 H	0.03854 O2	0.02132 NO
1.55E-02 O	2.06E-03 AlOCl	1.78E-03 AlHO2	4.52E-04 AlCl
3.15E-04 OCl	2.84E-04 AlCl2	2.34E-04 Cl2	1.46E-04 HOCl
1.29E-04 HO2	9.14E-05 AlHO	8.24E-05 AlCl3	7.27E-05 AlO
1.62E-05 COCl	1.13E-05 N	1.08E-05 NHO	9.87E-06 NO2
7.07E-06 CHO	6.50E-06 AlO2	3.01E-06 Al	2.81E-06 NOCl
2.56E-06 NH3	2.20E-06 NH	2.16E-06 N2O	2.07E-06 NH2

THE MOLECULAR WEIGHT OF THE MIXTURE IS 26.883

TOTAL HEAT CONTENT (298 REF) =1300.366 CAL/GM
SENSIBLE HEAT CONTENT (298 REF)=1100.598 CAL/GM

*****EXHAUST RESULTS FOLLOW*****

T(K)	T(F)	P(ATM)	P(PST)	ENTHALPY	ENTROPY	CP/CV	SGAMMA	RT/V	TCRE
2328.	3731.	1.00	14.70	-102.24	239.98	1.1983	1.0000	0.288	

DAMPED AND UNDAMPED SPEED OF SOUND= 2808.133 AND 2943.688 FT/SEC

SPECIFIC HEAT (MOLAR) OF GAS AND TOTAL= 11.021 11.713
NUMBER MOLS GAS AND CONDENSED= 3.4716 0.0869

1.39225 H2O	0.57646 HCl	0.56546 N2	0.44959 CO2
0.28530 CO	0.15652 H2	0.04492 Al2O3&	0.04191 Al2O3*

2.17E-02 Cl	1.25E-02 HO	8.23E-03 H	1.63E-03 O2
1.30E-03 NO	4.38E-04 O	7.30E-05 AlOCl	3.55E-05 AlHO2
2.89E-05 Cl2	9.35E-06 AlCl3	7.82E-06 AlCl2	7.22E-06 AlCl
6.18E-06 HOCl	5.73E-06 OCl	1.09E-06 HO2	

THE MOLECULAR WEIGHT OF THE MIXTURE IS 28.102

TOTAL HEAT CONTENT (298 REF) = 895.892 CAL/GM

SENSIBLE HEAT CONTENT (298 REF)= 737.771 CAL/GM

*****PERFORMANCE: FROZEN ON FIRST LINE, SHIFTING ON SECOND LINE*****

An exact method for determining throat conditions was used

The frozen & shifting STATE gammas for the throat are: 1.1967 1.1239

ISentropic EXponent shown below is the gamma for the chamber to throat PROCESS.

IMPULSE	IS	EX	T*	P*	C*	ISP*	OPT	EX	D-ISP	A*M.	EX	T	ADH
216.5	1.1991	2887.	11.96	4945.7			3.63	380.2	0.51251	1886.	449406.		
224.8	1.1282	2998.	11.84	5050.8	193.4	4.04	394.6	0.52340	2328.	571890.			

**** NEWPEP - Feb. 1990 ****

LIST OF REFERENCES

1. Dash, S.M., Wolf, D.E., Beddini, R.A. and Pergament, H.S., "Analysis of Two Phase Flow Processes In Rocket Exhaust Plumes," *Journal of Spacecraft and Rockets*, Vol. 22, May-June 1985, pp. 367-380.
2. Dash, S.M., "Analysis of Exhaust Plumes and Their Interaction with Missile Airframes," *Tacticle missile Aerodynamics*, AIAA Progress in Astronautics and Aeronautics, Volume 104.
3. Hermsen, R.W., "Aluminum Oxide Particle Size for Solid Rocket Motor Performance Prediction," *Journal of Spacecraft and Rockets*, Vol.18, No. 6, November-December 1981, pp. 483-490.
4. Nelson, H.F., "Influence of Particulates on Infrared Emission from Tactical Rocket Exhausts," *Journal of Spacecraft and Rockets*, Vol. 21, No 5, Sept-Oct. 1984, pp. 425-432.
5. Eno, T. J., *A Combined Optical and Collection Probe for Solid Propellant Exhaust Particle Analysis*, Master's Thesis, Naval Postgraduate School, Monterey, California, December 1989.
6. Misener, J.A., and Kessel, P.A., "Current AFRPL Measurements and Characterization of Particulates in Solid Rocket Motor Plumes," *15th JANNAF Plume Technology Meeting*, pp.275-284, CPIA Publication 426, May 1985.
7. Hovland, D.L., "Particle Sizing in Solid Rocket Motors," Master's Thesis, Naval Postgraduate School, Monterey, California, March 1989.
8. Pruitt, T.E., "Measurement of Particle Size Distribution a Solid Propellant Rocket Motor Using Light Scattering," Master's Thesis, Naval Postgraduate School, Monterey, California, June 1987.
9. Youngborg, E.D., "Application of Laser Diffraction Techniques to Particle Sizing in Solid Propellant Rocket Motors," Master's Thesis, Naval Postgraduate School, Monterey, California, December 1987.

10. *Mastersizer Instruction Manual*, Malvern Instruments LTD, Manual Version IM 100, Issue 3, October 1989, pp. 1.23-1.26.
11. *Instruction Manual for the Model S-450 SEM*, Hitachi Ltd, Japan, Part # 531-E250, Sept, 1977.
12. Lee, Y.L., "Particle-Sizing System for Scanning Electron Microscope Images of Solid Fuel Combustion Exhaust, : Master's Thesis, Naval Postgraduate School, Monterey, California, March 1991.

INITIAL DISTRIBUTION LIST

	No. of copies
1. Defense Technical Information Center Cameron Station Alexandria, Virginia 22304-6145	2
2. Library, Code 52 Naval Postgraduate School Monterey, California 93943-5002	2
3. Department Chairman, Code AA Department of Aeronautics and Astronautics Naval Postgraduate School Monterey, California 93943-5004	1
4. Professor D.W. Netzer, Code AA/Nt Department of Aeronautics and Astronautics Naval Postgraduate School Monterey, California 93943-5004	2
5. CPT L.J. Kellman P.O. BOX 799 Palo Alto, California 94302	2
6. David Laredo, Code AA Department of Aeronautics and Astronautics Naval Postgraduate School Monterey, California 93943-5004	1